universität wien

MASTERARBEIT / MASTER'S THESIS

Titel der Masterarbeit / Title of the Master's Thesis

Basic characterization of the hematopoietic system in type I interferon deficient mice

verfasst von / submitted by

Andrea Lorenz, BSc

angestrebter akademischer Grad / in partial fulfilment of the requirements for the degree of

Master of Science (MSc)

Wien, 2023 / Vienna, 2023

Studienkennzahl lt. Studienblatt / degree programme code as it appears on the student record sheet:	UA 066 830
Studienrichtung lt. Studienblatt / degree programme as it appears on the student record sheet:	Masterstudium Molecular Microbiology, Microbial Ecology and Immunobiology
Betreut von / Supervisor:	O.Univ.-Prof. Dr.med.vet. Mathias Müller

Statutory declaration

I hereby declare that this master's thesis has been written only by the undersigned and without any assistance from third parties. Furthermore, I confirm that no sources have been used in the preparation of this thesis other than those indicated in the thesis itself. I also state that all copyrights have been respected and met. Nonetheless, if infringements of any kind should emerge, I solicit you courteously to contact me first before taking any further (legal) actions.

Date _____ Signature _____

1 Table of contents

1 Table of contents 3
2 Abstract 5
3 Zusammenfassung 6
4 Introduction 7
4.1 Type I Interferons (IFN-I) 7
4.1.1 Interferon signaling 9
4.2 Development of hematopoietic cells in mice 10
4.3 The role of tonic IFN-I in hematopoiesis 12
4.4 Newly generated IFN-I mutant mice 14
5 Aim of this master's thesis 15
6 Materials and methods 16
6.1 Mice 16
6.1.1 Mouse strains 16
6.2 Blood and organ isolation 16
6.3 Flowcytometry 16
6.3.1 Isolation of splenic and thymic cells 16
6.3.2 Isolation of bone marrow cells 17
6.3.3 Antibody staining against surface markers 17
6.3.4 Staining panels 18
6.4 Organ homogenization and Western Blot 19
6.4.1 Sample preparation 19
6.4.2 Bicinchoninic acid (BCA) assay 19
6.4.3 SDS-PAGE and immunoblotting 19
6.4.4 Semi-dry transfer 20
6.4.5 Semi-quantification of protein levels 20
6.5 Luminex assay – bead-based multiplex assay 21
6.6 RNA isolation and RT-qPCR 22
6.6.1 TRIzol isolation and DNase treatment 22
6.6.2 Quality control 22
6.6.3 cDNA synthesis 23
6.7 Statistics 23
6.8 Resource Tables 23
6.8.1 PCR protocols and recipe 23
6.8.2 Primer for RT-qPCR 23

6.8.3 Antibodies for Flowcytometry 24
6.8.4 Antibodies for Western Blot 25
6.8.5 Table of abbreviations 26
6.8.6 Table of buffers 27
6.8.7 Table of reagents 28
6.8.8 Equipment and software table 29
6.9 Gating strategies for Flowcytometry 30
7 Results 32
7.1 Mice deficient in IFNα display reduced spleen weight and splenocyte numbers 32
7.2 Lack of IFN-I results in elevated numbers of erythroid and myeloid progenitor cells 33
7.3 Elevated levels of erythroid and myeloid progenitors result in unaltered mature immune cell populations 34
7.4 Reduction of lymphoid progenitor cells in IFN-I mutant mice has a low impact on mature T cells, B cells and DCs 35
7.5 IFN-I deficiency leads to decreased NK cell numbers and impaired NK cell maturation in the spleen 36
7.6 STAT1 protein levels are affected by lack of IFNα 37
8 Discussion 38
9 Acknowledgements 41
10 References 42

2 Abstract

Type I interferons (IFN-Is) have been known for their crucial role in antiviral defense and orchestration of the immune system. Interferonopathies emphasize the importance of proper regulatory mechanisms for these potent responders to danger. IFN-Is are constitutively expressed in healthy individuals, a process called tonic signaling, which maintains immune homeostasis. Even though the effects of tonic IFN-I signaling on hematopoiesis have been partially characterized in *Ifnar1*$^{-/-}$ and *Ifn*$\beta^{-/-}$ mice, we are for the first time able to dissect the functions of distinct members of the IFN-I family by analyzing mice deficient in IFNα, IFNβ or both. Using flowcytometric analyses we found a IFN-I-dependent reduction of common lymphoid progenitors (CLPs) and a pronounced IFNα-dependent decrease of the most mature (M2) NK cell subset. Furthermore, we report a reduction of total splenic NK cells in all IFN-I mutant mice, whereas other mature cells of the lymphoid and myeloid lineage in spleen, blood and bone marrow remain unaffected by loss of IFNα, IFNβ or both. These aberrations in NK cells were accompanied by a reduction of STAT1 protein levels in spleens of all IFN-I mutant mice and confirmed the previously shown regulation of STAT1 by tonic IFN-I signaling. STAT1 deficiency is known to lead to a similar, yet more severe NK cell phenotype, suggesting that the main driver of alterations in IFN-I mutant mice is dysregulation of STAT1.

3 Zusammenfassung

Typ I Interferone (IFN-I) sind für ihre zentrale Rolle in der antiviralen Abwehr und der Organisation des Immunsystems bekannt. Interferonopathien haben die Bedeutung einer angemessenen Regulation von IFN-I gezeigt. Geringe Mengen an IFN-I sind auch in gesunden Menschen dauerhaft nachweisbar. Die Auswirkungen dieser basalen Signale auf die Hämatopoese wurden bereits teilweise in *Ifnar1*- und *Ifnβ*-defizienten Mäusen beschrieben. Wir sind nun zum ersten Mal in der Lage, in Mäusen denen IFNα, IFNβ oder alle IFN-I fehlen, die Funktionen der verschiedenen Subtypen in der Bildung der Immunzellen unter homöostatischen Bedingungen zu untersuchen. Mittels durchflusszytometrischer Analysen haben wir gezeigt, dass die Reduktion von lymphoiden Vorläuferzellen von IFN-I abhängig und dass IFNα essenziell für die finale NK-Zell-Reifung ist. Des Weiteren konnten wir reduzierte NK-Zellzahlen in der Milz in allen IFN-I Mutanten feststellen, allerdings werden andere reife lymphoide und myeloide Zellen von IFN-I Defizienz nicht beeinträchtigt. In der Milz konnten wir zusätzlich zu den Veränderungen in NK-Zellen auch verminderte STAT1 Proteinmengen nachweisen und dadurch den bekannten Einfluss basaler IFN-I Signale auf die Regulation von STAT1 bestätigen. Ein Fehlen von STAT1 resultiert in einem ähnlichen, jedoch schwerwiegenderen NK-Zell Phänotyp. Demnach postulieren wir die Dysregulierung von STAT1 als hauptverantwortlich für die im Rahmen dieser Arbeit vorgestellten Veränderungen in NK-Zellen von IFN-I-defizienten Mäusen.

4 Introduction

Interferons (IFNs) are a conserved group of cytokines found in vertebrates and function as important signaling molecules in infections (Borden et al. 2007). They were discovered in 1957 as factors interfering with viral replication (Isaacs and Lindenmann 1957) and in the following decades more and more members of the IFN family were identified, their functions described and the mechanism behind their signaling unraveled (Borden et al. 2007). IFNs are involved in antiviral and antimicrobial defense, differentiation of immune cells, stimulation of the immune system, promotion of antitumor activities, antiproliferative activities, induction of apoptosis and senescence (Schreiber 2017).

IFNs are categorized into three types: the type I IFN (IFN-I) family with the main representatives being various subtypes of IFNα and IFNβ; the single IFN-II, called IFNγ (Borden et al. 2007); and the IFN-III family which in mice is comprised of IFN-λ2, IFN-λ3 and two pseudogenes (Kotenko et al. 2019).

Even though both IFN-Is and IFN-II are involved in anti-viral defense, their mode of action differs. IFN-Is act predominantly by activating the cell-intrinsic defense mechanisms of possible target cells, also called the anti-viral state. IFN-II in contrast mainly activates macrophages and thereby increases their ability to clear ingested intracellular, non-viral pathogens (Decker, Müller, and Stockinger 2005). IFN-IIIs have similar functions to IFN-Is, although they are mostly produced by epithelial cells and exert their functions preferentially on mucosal surfaces (Kotenko et al. 2019).

4.1 Type I Interferons (IFN-I)

The IFN-I family in mice consists of one IFNβ, 14 different IFNα subtypes, multiple limitins (IFNζ) and one IFNε (Decker, Müller, and Stockinger 2005), all of which are encoded in the IFN-I-cluster on mouse chromosome 4 (Figure 1). IFNκ, another member of the IFN-I family, is encoded on the same chromosome, but situated outside of this cluster (Hardy et al. 2004). IFN-Is are encoded by conserved and, except for IFNκ, are intronless genes and the presence of some subtypes differ between species (Borden et al. 2007).

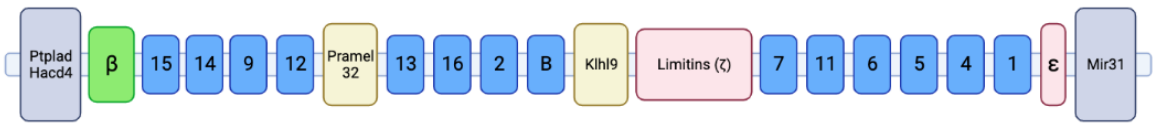

Figure 1: ***Scheme of type I interferon cluster on mouse chromosome 4.*** *IFNα subtypes are depicted in blue, IFNβ in green, other IFN-Is in red, protein-coding non-IFN genes in yellow and genes used as margins for this locus are depicted in grey. Created with BioRender.com*

IFN-Is can be produced by almost all cells, with the main producing cell types being plasmacytoid dendritic cells (pDC) (Borden et al. 2007), macrophages (Fleetwood et al. 2009) and stromal cells (Swiecki and Colonna 2011). Due to the ubiquitous expression of their receptor, virtually all cells in the body can be affected by IFN-Is (Borden et al. 2007).

IFNα and IFNβ are the best studied representatives of the IFN-I family. However, IFNα subtypes are rarely distinguished, even though they differ in their function due to distinct receptor affinities, and their divergent patterns and kinetics of induction (Fox, Locke, and Lenschow 2020). An important difference between IFNα and IFNβ is their dependency on the transcription factors interferon regulatory factor (IRF) 3 and 7. While IFNβ and IFNα4 can be induced in the presence of constitutively expressed IRF3 alone, all other IFNαs additionally require the presence of IRF7. This transcription factor is only induced downstream of IFN signaling, except in pDCs, which express IRF7 constitutively, making them the ideal producers of IFNα (Fox, Locke, and Lenschow 2020). Furthermore, IRF3 and IRF7 are regulated by IFN-Is, thereby forming an autocrine loop, which enables the rapid and robust expression of IFN-Is upon induction. (Gough et al. 2012).

IFN-Is are induced upon sensing of motifs associated with cellular damage or presence of microbes, most commonly nucleic acids and microbial cell-wall components. These motifs are recognized by pattern recognition receptors, such as Toll-like receptors (TLRs), C-type lectin-like receptors (CLRs), retinoic acid-inducible gene I (RIG-I)–like receptors (RLRs), NOD-like receptors (NLRs) and cGAS-STING (Yu and Liu 2021).

IFN-Is are produced constitutively in vanishingly small quantities (van Pesch and Michiels 2003). This low-level expression is termed tonic IFN-I and is stimulated by commensal microbes, especially in the gut (Schaupp et al. 2020). This small amount of IFN-Is is needed to prepare the cells to react more vigorously to possible stimuli by maintaining low levels of expression of IFN-I target genes. However, the levels are too low to activate the positive feedback loop and thereby do not enhance IFN-I production any further (Takaoka et al. 2000).

Tonic signaling differs from induced signaling by the transcription factors that are involved. While induced IFNβ signaling relies on IRF3 and IRF7, tonic signaling has been described to be dependent on specific components of AP-1 and NF-κB and is further characterized by involvement of IRF2 and p50 dimers as repressors (Gough et al. 2012). Examples of important processes that are disturbed in the absence of tonic IFN-I signaling are the responses to IFNγ, interleukin 6 (IL-6) and also to IFN-I itself (Taniguchi and Takaoka 2001).

IFN-Is exert both beneficial and detrimental effects in viral, bacterial, and parasitic infections depending on the tissue and the specific pathogen. In viral infections IFN-Is elicit the antiviral state and additionally have roles in DC maturation, augmenting antibody production and improving cytolytic T cell functions. IFNα has been described to be important to limit viremia and viral dissemination, while the effects of IFNβ are more diverse and include also detrimental effects (Fox, Locke, and Lenschow 2020).

In bacterial infections IFN-Is have ambivalent roles and their effects differ according to pathogen, route of infection and dissemination of the microbe. For example, IFN-I have protective effects in lung infections with *Streptococcus pneumoniae* and *Legionella pneumophilia* (Kovarik et al. 2016), whereas they exert a detrimental impact in systemic *Listeria monocytogenes* infections (Kernbauer et al. 2013).

Aberrant stimulation or defective negative regulation of the IFN-I system can result in IFN-I overproduction which leads to severe pathologies, called interferonopathies. These are considered as autoimmune diseases, with Aicardi–Goutières syndrome and certain forms of systemic lupus erythematosus as the most prominent examples (Crow and Stetson 2022).

4.1.1 Interferon signaling

All IFN-Is signal through the IFNα/β receptor (IFNAR), which consists of the two subunits IFNAR1 and IFNAR2 (Borden et al. 2007) (Figure 2, left). These subunits are associated with members of the Janus kinase (Jak) family, namely tyrosine kinase 2 (Tyk2) and Jak1. Upon IFN-I binding, the receptor components, including their respective Jaks, associate with each other and enable Jak dimerization. The Jaks subsequently phosphorylate each other (trans-phosphorylation) and thereby stimulate each other's kinase activity, enabling phosphorylation of the receptors (Caveney et al. 2023). This allows recruitment of the signal transducers and activators of transcription (STAT) 1 and 2, which in turn are phosphorylated at their C-terminal tyrosine residues by the appropriate Jaks (Gough et al. 2010). Activated STAT1 and STAT2 can form homo- or heterodimers. The heterodimers bind to IRF9 to form the IFN-stimulated gene factor 3 (ISGF3), which subsequently translocates to the nucleus and binds to IFN-stimulated response elements (ISRE) on the DNA. STAT1 homodimers directly bind to DNA at gamma IFN-activated sites (GAS). Finally, interaction with ISRE and GAS leads to transcription of numerous IFN stimulated genes (ISGs) (Platanias 2005).

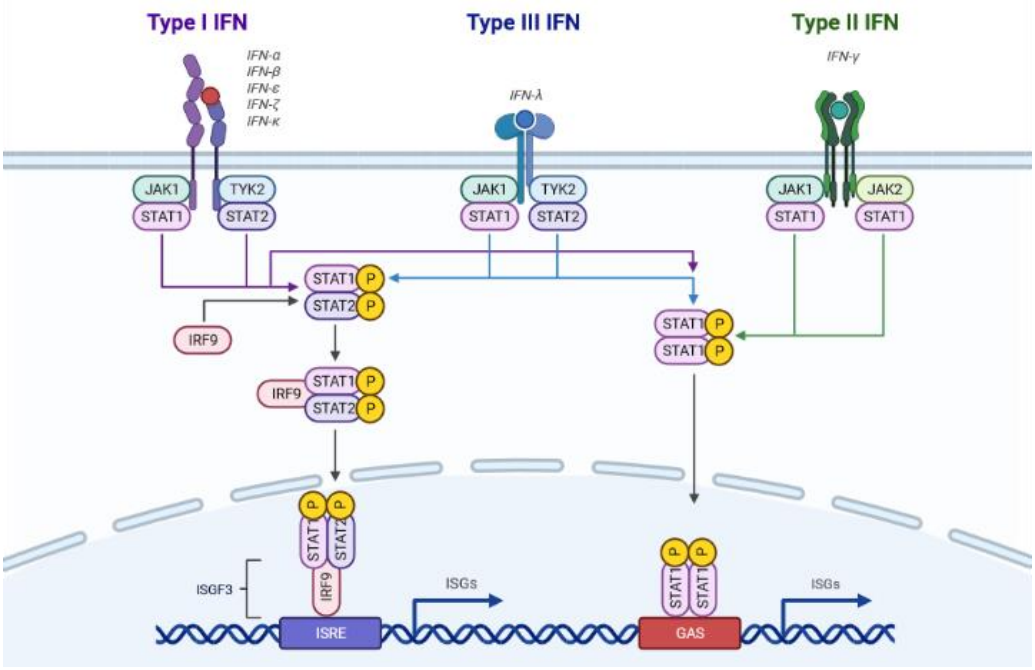

Figure 2: ***Transduction of interferon (IFN) signaling****. JAK 1/2 – Janus kinase 1/2, TYK2 – tyrosine kinase 2, STAT1/2 - signal transducer and activator of transcription 1/2, IRF9 – interferon regulatory factor 9, ISGF3 – interferon stimulated gene factor 3, ISRE – interferon-stimulated response element, GAS – gamma activated sequence, ISGs – IFN stimulated genes, P – phosphate; created in BioRender.com*

IFN-II signals through the heterodimeric IFNγ-receptor, which is composed of two IFNGR1 and IFNGR2 chains and is activated by IFNγ (Figure 2, right). While IFNGR1 is constitutively expressed on all cells, its partner IFNGR2 is tightly regulated and expressed more scarcely. Similarly to IFN-Is, IFN-II activates Jak1, however the second kinase involved is Jak2 (Borden et al. 2007).

IFN-IIIs resemble IFN-Is not only in function, but also in their mode of signaling (Figure 2, middle). The receptor for IFN-IIIs consists of IFN-λR1 and IL-10R2 and its downstream signaling is mediated via Jak1 and Tyk2, which phosphorylate STAT1 and STAT2 (Kotenko et al. 2019).

4.2 Development of hematopoietic cells in mice

The generation of blood cells in mammals is a hierarchical, yet continuous process with hematopoietic stem cells (HSCs) as their origin (Zhang et al. 2018). Numerous progenitors originate from them and then differentiate stepwise into all the mature hematopoietic cells (Figure 3). Even though the view on the hematopoietic hierarchy changed in recent years, adding intermediate-term HSCs (IT-HSC) and subsets of multipotent progenitors (MPPs), the concept of a self-renewable hematopoietic stem and progenitor cell compartment, gradually differentiating into lineage determined offspring, remained the same (Zhang et al. 2018). In this study we will use a simplified depiction of an older model, as it illustrates all the populations analyzed later in this thesis.

The MPPs are the first population arising from the HSCs and differentiate in the bone marrow (BM) into the lineage specific megakaryocyte-erythroid progenitors (MEPs), common myeloid

progenitors (CMPs), lymphoid-myeloid primed progenitors (LMPPs) or common lymphoid progenitors (CLPs) (Belyavsky, Petinati, and Drize 2021). MEPs are the source of the megakaryocyte and the erythroid lineage and therefore generate megakaryocyte progenitors (MkPs) and erythroblasts, which in turn produce platelets and erythrocytes, respectively (Lu et al. 2018). The CMPs can differentiate into either MEPs or granulocyte-macrophage progenitors (GMPs), the latter subsequently give rise to granulocytes, monocytes, and macrophages.

As progenitors of the lymphoid lineage, CLPs give rise to natural killer (NK) cells and immature B and T cells, which mature in secondary lymphoid organs and in the thymus respectively (Belyavsky, Petinati, and Drize 2021). LMPPs generate common dendritic precursors (CDPs), which terminally differentiate into DCs.

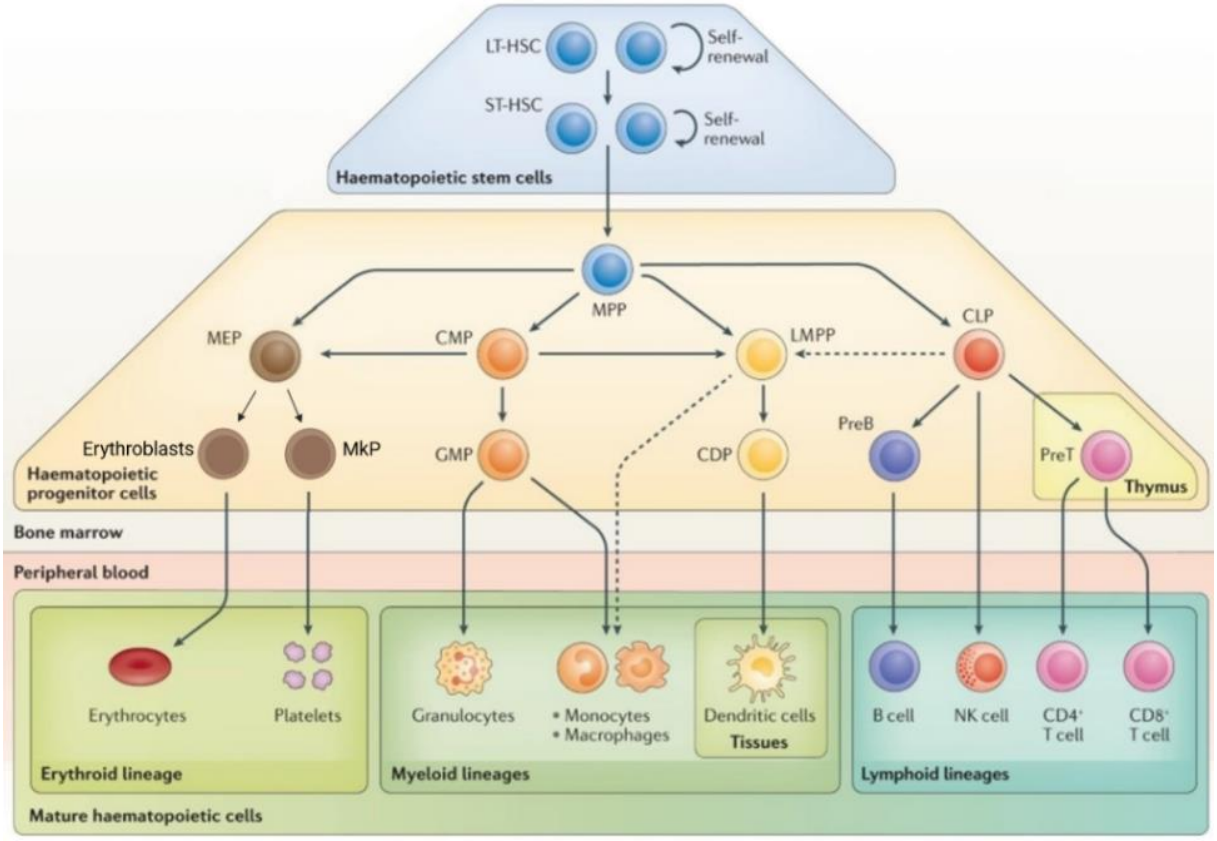

Figure 3: ***The hematopoietic hierarchy.*** *Blood cells develop from hematopoietic stem cells via lineage-specific progenitor cells into the mature populations of the erythroid, myeloid, and lymphoid lineage. LT-HSC – long-term hematopoietic stem cells, ST-HSC – short-term HSC, MPP – multipotent progenitors, MEP – megakaryocyte-erythrocyte progenitors, MkP – megakaryocyte progenitors, CMP – common myeloid progenitors, GMP – granulocyte-macrophage progenitors, LMPP – lymphoid-myeloid primed progenitors, CDP – common dendritic precursors, CLP – common lymphoid progenitors; Adapted from (Ferrari, Thrasher, and Aiuti 2021) with BioRender.com*

4.3 The role of tonic IFN-I in hematopoiesis

IFN-Is are known to have strong effects on hematopoietic cells during infections. However, even in homeostasis IFN-Is were shown to be expressed in small quantities and are important for maintenance of various immune cell populations (Tovey et al. 1987).

The interest in studying functions and effects of IFN-Is arose in the early 1990s and lead to the generation of two *Ifnar1*$^{-/-}$ mouse models (Müller et al. 1994; Hwang et al. 1995). The main focus of research was on the role of IFN-Is in infection. However, the basic characterization of these mice revealed that IFN-Is interfere with the development of mature hematopoietic cells of the myeloid lineage under homeostatic conditions. Compared to their control littermates, *Ifnar1*-deficient mice showed increased levels of neutrophils and macrophages in the BM (Hwang et al. 1995) and of circulating mature monocytes, macrophages and neutrophils in the blood (Müller et al. 1994; Hwang et al. 1995).

The impact of tonic IFN-I signaling on stem and progenitor cells is still unclear. It is known that HSCs react to induced IFN-I by exiting quiescence (Essers et al. 2009) and prolonged exposure leads to their exhaustion (Sato et al. 2009). A reduction in the overall hematopoietic stem and progenitor cell (HSPC) compartment, defined as Lineage^{-}Sca-1^{+}c-KIT^{+} (LSK) cells was described in *Ifnar1*$^{-/-}$ mice (Gui et al. 2017). Levels of HSCs were described to be slightly reduced (Essers et al. 2009; Gui et al. 2017) or similar to wild type (WT) levels (Li et al. 2023).

Two studies described decreased numbers of NK cells upon loss of IFN-I signaling (Swann et al. 2007; Mizutani et al. 2012). The reduction in NK cells was proposed to be caused by a downregulation of the IFN-I-regulated cytokine IL-15, which NK cells need for their proliferation (Kennedy et al. 2000; Mattei et al. 2001). However, later studies did not find differences in NK cell abundance when compared to WT (Guan et al. 2014; Meissl et al. 2020). An impaired NK cell maturation, characterized by alterations in expression of the surface markers CD27 and CD11b, was described (Mizutani et al. 2012; Meissl et al. 2020). Furthermore, reduced NK cell cytotoxicity was documented (Mizutani et al. 2012).

Loss of IFN-I leads to a reduction in the pre-pro B cell subset (Mizutani et al. 2012), but no alterations in more mature B cells were detected (Vasconcellos et al. 1999; Mizutani et al. 2012). Furthermore, a shift to more multi-reactive B cells in the BM and thymus of *Ifnar1*$^{-/-}$ mice has been described (Vasconcellos et al. 1999).

Mice deficient in IFNAR2 have been generated, however no detailed analyses on the development of their immune cells were published (Fenner et al. 2006; Shepardson et al. 2018).

As the interest in dissecting the effects of different IFN-I subtypes increased, three independent *Ifnβ*$^{-/-}$ mouse models were generated (Erlandsson et al. 1998; Takaoka et al. 2000; Deonarain et al. 2000).

Ifnβ$^{-/-}$ mice display an impaired B cell maturation, resulting in reduced pro-B, pre-B and mature B cells in the BM (Deonarain et al. 2003). Studies on earlier B cell lineage development described a strong reduction in the early pro-B cells, but could not corroborate the differences in the abundance of all later stages of B cell development in the spleen or lymph nodes (Mizutani et al. 2012). Together with data on reduced pre-pro B cells in *Ifnar1*$^{-/-}$ mice they suggested IFN-Is to impact the earliest stages of B cell development, specifically between CLPs and the early pro-B cell transition.

Loss of IFNβ results in strongly reduced colony-forming units granulocyte-monocyte (CFU-GM) in the BM, while on burst-forming units erythroid (BFU-E) and CFU-granulocyte-erythroid-macrophage-megakaryocyte (GEMM) only minor effects were reported. Due to this reduction of myeloid progenitors, *Ifnβ*-deficient mice also displayed reduced levels of macrophages in BM and blood and decreased circulating neutrophils (Deonarain et al. 2003).

CD4^{+} and CD8^{+} T cell abundance and proportion have been described to be similar to WT in *Ifnβ*$^{-/-}$ and *Ifnar1*$^{-/-}$ mice (Deonarain et al. 2003; Müller et al. 1994).

So far, no *Ifnα*-deficient mouse has been generated, mainly due to the technical difficulty of deleting the more than 300kb of DNA comprising the IFN-I-cluster. Consequently, IFNα specific effects could not be observed directly so far.

4.4 Newly generated IFN-I mutant mice

Christian Schindler (Columbia University, NY) generated a set of four mouse lines (three IFN-I mutants and the corresponding WT control (IFN-I$^{fl/fl}$)) to elucidate the contributions of IFNα and IFNβ to the overall IFN-I response (Figure 4). Mutants lacking the entire IFN-I locus including all IFNα subtypes, IFNβ, IFNε, IFNζ, Klhl9 and Pramel32 are referred to as IFN-I$^{-/-}$ mice. *Ifnα*$^{-/-}$ mice retain only the *Ifnβ* gene, while *Ifnβ*$^{-/-}$ mice retain the entire IFN-I cluster, except the *Ifnβ* gene. IFNκ is not located in the IFN-I cluster and therefore remains present in all mutants. The two non-IFN genes *Pramel32* (ENSMUSG00000038330) and *Klhl9* (ENSMUSG00000070923; Chen et al. 2014), which are located in the locus are deleted in the *Ifnα*$^{-/-}$ and the IFN-I$^{-/-}$ mice. KLHL9 is part of Cul3-RING ubiquitin ligase complex and thereby involved in ubiquitin-protein transferase activity. Pramel32 is predicted to be part of Cul2-RING ubiquitin ligase complex and to be expressed in ovaries of adult mice.

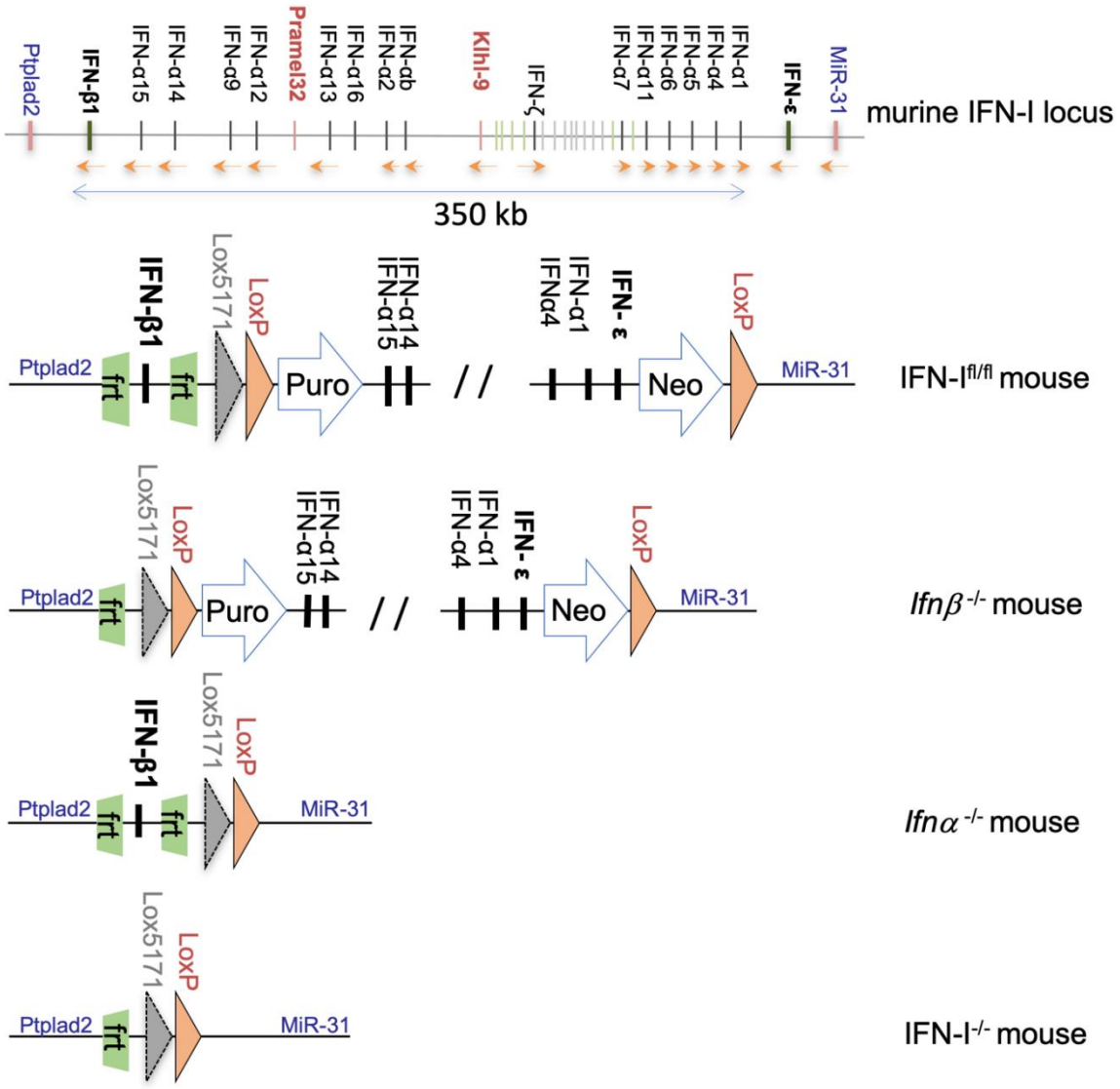

Figure 4: ***Scheme of the murine IFN-I locus and IFN-I mutant mice.*** *Puro = puromycin/Neo = neomycin (selection markers); LoxP & frt = recognition sites for Cre-recombinase and flippase respectively; Ptplad2 and MiR-31 serve as margins for this locus (this scheme was kindly provided by Christian Schindler)*

5 Aim of this master's thesis

The aim of this project is the basic characterization of the newly generated IFN-I mutant mice during homeostasis. Abundance of various immune cells will be determined by Flowcytometry and compared between mouse lines. Hence distinct functions of IFNα and IFNβ in hematopoiesis may be revealed.

6 Materials and methods

6.1 Mice

IFN-I$^{fl/fl}$, *Ifnα*$^{-/-}$, *Ifnβ*$^{-/-}$ and IFN-I$^{-/-}$ mice (on mixed C57BL6/J and C57BL6/N background; Table 6.1.1) were bred at the University of Veterinary Medicine Vienna under specific-pathogen-free (SPF) conditions according to Federation of European Laboratory Animal Science Associations (FELASA) guidelines.

6.1.1 Mouse strains

Strain	Official name
IFN-I$^{fl/fl}$	B6.Cg-IFNalphabeta$^{<tm1.shnd>}$
IFN-I$^{-/-}$	B6.Cg-IFNalphabeta$^{<tm1.3shnd>}$
Ifnα$^{-/-}$	B6.Cg-IFNalphabeta$^{<tm1.1shnd>}$
Ifnβ$^{-/-}$	B6.Cg-IFNalphabeta$^{<tm1.2shnd>}$

For Flowcytometry 8–12-week-old mice were used, while for RT-qPCR and Western Blot analysis mice up to 15 weeks of age were included. In flowcytometric analyses mostly female mice were used, if not enough females were available, males were included, which in the end resulted in 2-4 out of 15 individuals, depending on the genotype. For RT-qPCR and Western Blot, both male and female mice were used.

6.2 Blood and organ isolation

Mice were anaesthetized by intraperitoneal injection of Ketamine/Xylazine (100 mg/kg body weight Ketamine, 4 mg/kg body weight Xylazine) and retrobulbar blood sampling was performed with a sterile hematocrit capillary tube into EDTA tubes for basic hematological analysis via VetABC. Afterwards mice were sacrificed by CO_2 and/or cervical dislocation and spleen, thymus, liver, and hind legs were isolated and transferred to the appropriate buffer solutions for further analysis.

6.3 Flowcytometry

6.3.1 Isolation of splenic and thymic cells

Isolated spleen (whole organ or a piece of it) was transferred in 500µl RPMI and subsequently placed in a 12-well plate and digested by injecting 1ml of digestion mix (Table of buffers 6.8.6.) with a needle into the spleen. Then the spleen was cut into small pieces and incubated for 30 min at 37°C in an incubator. Afterwards the spleen was further fragmented by pipetting with a 1ml micropipette with a cut tip. The digested fragments were transferred onto a 100µm MACS Smart strainer (Miltenyi) and pushed through the strainer with the plunger of a syringe into a 50ml tube. The tube was then filled up to 10ml with cold FACS buffer (Table of buffers 6.8.6.) to wash the strainer and

another 10ml were added to inactivate the digestion mix. Afterwards the cell suspensions were centrifuged at 400 x g for 5 min at 4°C.

For preparations without digestion spleen and thymus were stored in PBS and cells were isolated by pushing the organ through a 100µm strainer with the plunger of a syringe into a 50ml tube and subsequently washing the filter with 10ml of FACS buffer. Afterwards the cell suspensions were centrifuged at 400 x g for 5 min at room temperature (RT). These specifications were used for all following centrifugation steps in flowcytometric analyses.

From this step on, both preparations were treated the same. Red Blood Cell Lysis (RBC) was performed by resuspending the pellet in 1ml RBC lysis buffer and incubating for 5 min at RT. Then FACS buffer was added up to 10ml and the cells were centrifuged again, the pellet was resuspended in 2ml FACS buffer and subsequently passed through another 100µm cell strainer, which was then washed with another 8ml of FACS buffer to reach a total volume of 10ml. The 10ml cell suspension was then counted in a BioRad TC20 automated cell counter, and 5 million cells were used for staining. To obtain immune cells from blood, red blood cell lysis was performed twice, and all cells were taken for staining.

6.3.2 Isolation of bone marrow cells

Both hind legs were removed and stored on ice in 50ml tubes filled with PBS. Skin, foot, and knee were cut before removing muscles and tendons with a tissue. After cleaning, the bones were stored in fresh, cold PBS.

For isolation of cells used for HSPC staining femur and tibia were ground in a mortar with 2ml of FACS Buffer into small pieces. These pieces were then transferred onto a 100µm cell strainer and cells were pushed through it with the plunger of a syringe.

Cells used for lymphoid, myeloid and erythroblast staining were obtained by cutting both ends of the femur and rinsing out the BM with FACS buffer and a needle into a 50ml tube. The BM was subsequently resuspended with a 5ml pipette.

Afterwards red blood cell lysis, filtering and counting were performed in the same way as for splenocytes.

6.3.3 Antibody staining against surface markers

5 million cells were spun down at 400 x g for 5 min, resuspended in 50µl of the respective staining solution (Staining panels) and incubated for 20 min protected from light at 4°C. Afterwards the cells were washed with 2ml FACS buffer, centrifuged again. Pellets were mixed carefully, before adding 250µl of fixation buffer. After incubation for 15 min at RT in the dark, cells were washed with

2ml FACS buffer again, resuspended in 200µl of FACS buffer and stored in the fridge over night or analyzed right away.

2-3 million cells were recorded per sample, except for cells from blood and the hematopoietic stem and progenitor cell panel, where all available cells and 6 million cells were recorded, respectively.

6.3.4 Staining panels

- Staining panel for myeloid cells

  FCγ-block, viability dye (APC-Cy7), F4/80 (FITC), Ly6C (PerCP-Cy5.5), CD11c (APC-AF700), Ly6G (PE-610), MHC II (PE), lineage: NK1.1, CD3e, Ter-119, B220 (PE-Cy7), CD11b (PB)

- Staining panel for lymphoid cells

  FCγ-block, viability dye (APC-Cy7), CD27 (FITC), CD11b (PerCP-Cy5.5), CD19 (APC), CD3 (PE-610), CD4 (PE), NK1.1 (PE-Cy7), CD8 (PB)

- Staining panel for blood cells

  FCγ-block, viability dye (APC-Cy7), Ly6G (FITC), B220 (Per-CP-Cy5.5), Ter-119 (APC-Cy7), CD8a (APC), NK1.1 (PE), CD11b (PE-Cy7), mouse IgM (PB), CD3 (KO525), CD4 (SB610)

- Staining panel for erythroblasts

  FCγ-block, viability dye (APC-Cy7), CD44 (PE), Ter-119 (PB)

- Staining panel for thymocytes

  FCγ-block, viability dye (KO525), CD69 (FITC), CD25 (PerCP-Cy5.5), CD24 (APC-Cy7), CD45 (APC-AF700), CD44 (PE), CD8a (PE-Cy7), TCR beta (PB), CD4 (SB60)

- Staining panel for hematopoietic stem and progenitor cells

  Viability dye (KO525), CD150 (FITC), CD16/32 (PerCP-Cy5.5), cKIT (APC-Cy7), CD45 (APC-AF700), CD34 (APC), CD127 (PE-610), CD135 (PE), SCA-1 (PE-Cy7), lineage: CD11b, Ly-6G/Ly-6C, CD3e, Ter119, F4/80 (PB), CD48 (SB610)

- Staining panel for dendritic cells

  FCγ-block, viability dye (KO525), CD11b (FITC), Ly6C (PerCP-Cy5.5), MHC II (APC-Cy7), CD11c (APC-AF700), B220 (APC), CD8a (PE), BST2 (PE-Cy7), lineage: NK1.1, CD3e, Ter119 (PB), CD4 (SB610)

6.4 Organ homogenization and Western Blot

6.4.1 Sample preparation

Organs for Western Blot were harvested and either shock-frozen in liquid nitrogen or immediately homogenized. For homogenization the organs were placed in an 2ml round-bottom tube containing 1ml of Schindler buffer (Table of buffers 6.8.6.) and 2 magnetic beads. The tubes were placed in the 1600 Spex MiniG Tissue Homogenizer and homogenized for 1 min at 1500rpm. After 20 min of incubation on ice, the cell debris was removed by centrifugation for 5 min at 16100 x g at 4°C. The supernatant was subsequently transferred to a new tube.

6.4.2 Bicinchoninic acid (BCA) assay

Protein concentration was determined with the Pierce™ BCA Protein Assay Kit by Thermo Scientific and performed according to the manufacturers protocol. The BSA standard provided in the kit was diluted in PBS to a concentration between 25 and 2000µg/ml. The samples were diluted 1:10 in PBS in order to be in the working range of the assay and to avoid interference of the Schindler buffer with the assay.

The provided reagents A and B from the kit were mixed in the indicated ratio of 50:1 to prepare the working reagent. 25µl of samples and standards were pipetted into a 96-well flat bottom microplate with a lid (Falcon) on ice, each of them in duplicates, before adding 200µl of working reagent to each well and mixing them by carefully tapping the plate and incubating it for 30 min at 37°C. Afterwards the absorbance at 562nm was measured in a plate reader in technical duplicates. The average absorbance for each sample was calculated, the value of blank was subtracted, and the standard curve was calculated.

The concentration of the samples was determined using this curve and the concentration was adjusted to 10µg/µl with Schindler buffer, before adding 5x Lämmli sample buffer. These samples were then incubated for 5 min at 96°C and spun down for 1 min at 16100 x g at 4°C, before storing them at -20°C, while the original lysates were stored at -80°C.

6.4.3 SDS-PAGE and immunoblotting

An 8% separating gel with a 5% stacking gel on top, with a thickness of 1mm, was cast into a BioRad MiniGel apparatus. The samples were again heated to 96°C for 5 min and then centrifuged for 1 min at 16100 x g at 4°C, before loading 8µg of protein and 5µl of Thermoscientific PageRuler pre-stained protein ladder (diluted 1:2) onto the gel. Gels were run for approximately 2h starting with 80V and subsequently increasing to 120V, when the proteins have reached the separating gel.

6.4.4 Semi-dry transfer

After running the gel, it was removed from the glass plates and the bromophenol blue front, and the stacking gel were cut off. The remaining separating gel and the nitrocellulose membrane (8.4cm x 5.7cm) were equilibrated in transfer buffer.

In the semi-dry blotting apparatus, the blotting sandwich was assembled, by soaking Whatman paper and placing it on the bottom of the machine. Next, the equilibrated membrane was added, with the minimal amount of direct contact that is necessary for placing it there. Subsequently, the gel was added and covered with another layer of Whatman paper. The assembled sandwich was then rolled with a gel roller to remove any air bubbles between the membrane and the gel. Afterwards the apparatus was closed, and the transfer was performed with 1mA per cm^2 for approximately 2h. When the transfer was finished the membranes were washed in TBST before incubating them in approximately 3ml of Ponceau solution for 2 min. The Ponceau stain was washed out with TBST until distinct bands were visible. After taking a picture of the bands the nitrocellulose membrane was washed and incubated for at least 1h in blocking solution. Subsequently, the membrane was washed 3 times for 10 minutes in TBST before incubating in the primary antibody overnight at 4°C on a shaker. In order to detect the target protein and the loading control simultaneously, the membrane was cut slightly below the 70kDa marker of the PageRuler. After removing the primary antibody, the membranes were washed again three times for 10 min, then the secondary antibody was added at a concentration of 1:4000 for 1h at RT on a shaker. Afterwards the membranes were washed again three times with TBST and one time with TBS before recording the fluorescence pattern in an odyssey imager with recording intensity 5.

6.4.5 Semi-quantification of protein levels

The semi quantification of the STAT1 and STAT2 protein detection was performed via ImageJ on the black-and-white TIF files received from the imager. For each organ the most suitable intensity was determined to ensure comparability of the results. The file was opened in ImageJ and a region of interest (ROI) was defined for each protein, which corresponds to the minimum square necessary to contain the largest band of that protein. Afterwards the ROI was used to measure the mean grey value of every band and of the background above or below the band. These steps were performed for the STAT proteins as well as for the actin, which serves as a loading control with separate ROIs. Next, the inverted value was determined by subtracting the measurement from 255, which is the maximal possible value. Then the net value was calculated by subtracting the background value from the value of the band. Lastly, the ratio of protein of interest to loading control is determined.

6.5 Luminex assay – bead-based multiplex assay

The shock-frozen spleens and livers were homogenized in ProcartaPlex cell lysis buffer by Invitrogen (5µl per mg tissue) with two magnetic beads in the Spex 1600 MiniG Tissue Homogenizer at 1500rpm for 30 seconds. After removing the beads, the lysates were sonicated for 1 min at 35kHz, left on ice for 5 to 10 min before centrifugation at 16100 x g at 4°C for 10 min and subsequently, transferring the lysates into new tubes and determining the protein concentration via BCA assay.

All samples were diluted to a final concentration of 10mg/ml and this concentration was confirmed by a second BCA assay. Afterwards samples from the liver were diluted 1:3 for this analysis, while samples of the spleen were diluted 1:10. From there on the Luminex assay was performed according to the manufacturer's instructions in the ProcartaPlex Mouse Basic Kit. Standard Mix 1B (for IFNα) and IFNβ Standard were prepared by dissolving them in 250µl of universal assay buffer and combining aliquots of them. Then a 2.5-fold serial dilution in universal assay buffer was performed, creating 11 standards and one blank.

The wash buffer should have RT and needs to be diluted 1:10 before usage. To prepare the bead mixture, 1µl of each bead was added for every well and then filled up with wash buffer to a total of 50µl per well. The plate was placed on a hand-held magnetic washer and 50µl of the bead mix were added to each well. After 2 min, within which the beads should have attached to the magnet on the bottom of the plate, the plate was inverted to remove the wash buffer. After that, the beads were washed by adding 150µl of wash buffer to each well and inverting after 30 seconds. Subsequently, 25µl of universal assay buffer were added to each well in addition to 25µl of standard or sample (or universal assay buffer in case of the blank). Afterwards the plate was sealed with transparent plastic film, covered with a black lid, and incubated for 30 min at 500rpm at RT before incubating on 4°C overnight without shaking.

On the next day the antibody mixture was prepared by mixing 0.5µl of each detection antibody per well and filling up to 25µl per well with detection antibody diluent from the kit. The plate was removed from the fridge, placed on the magnetic washer, the seal was removed, and the plate was inverted. Afterwards a wash step was performed by adding 150µl of wash buffer and inverting after 30 seconds 3 times respectively. From here on this will be referred to as a wash step. Then the detection antibodies were added, the plate was sealed, removed from the washer, covered, and incubated for 30 min at 500rpm at RT. After the incubation, the plate was washed, before adding 50µl of Streptavidin-PE to each well, sealing, removing from the washer, covering, and incubating again for 30 min at 500rpm at RT. To prepare the plate for analysis, another wash step was performed, 120µl of reading buffer were added to each well and the plate was sealed and covered

again. Directly before putting the plate into the instrument, the plate was placed on a shaker and immediately before reading the seal was removed.

6.6 RNA isolation and RT-qPCR

6.6.1 TRIzol isolation and DNase treatment

One third of the spleen, one equally sized piece of liver and half of the thymus were placed in 300µl RNA-later solution and stored overnight on 4°C. The next day the organs were homogenized in 1ml TRIzol 3 times in 30 second intervals at 1500rpm in the 1600 Spex MiniG Homogenizer. Afterwards the beads were removed, and the samples were incubated for 5-10 min on RT. The samples were diluted 1:2 in TRIzol and the isolation was continued with 1ml of the homogenate. 200µl of chloroform were added to the sample, before shaking the tubes for 10-20 seconds by hand, incubating for 2 min at RT and centrifuging for 15 min at 4°C at 12000 x g. Then the aqueous upper phase was transferred into a new tube and diluted 1:2 with isopropanol to precipitate the RNA. After mixing the samples, we incubated for 10 min at RT and centrifuged for 10 min at 4°C at 12000 x g. Then, the supernatant was removed, and the RNA was washed twice in cold 75% Ethanol. Afterwards the pellet was allowed to dry and was then dissolved in nuclease-free water after rehydrating the pellet for 30 min. The concentration and purity of RNA was then determined via Nano Drop.

DNase treatment was necessary, which was performed with the RQ1 RNase-Free DNase kit by Promega. 1.5µg of RNA was mixed with 1.5µl of DNase and the reaction buffer in a total volume of 15µl of reaction mix. The samples were incubated for 30 min at 37°C before adding 1µl of DNase stop solution and incubation for 10 min at 6°C. Afterwards 10µl of the digestion was used for cDNA synthesis.

6.6.2 Quality control

RNA concentration was determined via Nano Drop. The ratios of the absorbance at 260nm/230nm and 260nm/280nm are indicators of contaminations and were used as means of quality control. For 260/230, ratios of 1.5 or higher and for 260/280, ratios of 1.8 or higher were considered acceptable. Additionally, an agarose gel was run to determine the degree of RNA degradation. If 2 out of those 3 criteria were met, the sample was included in the RT-qPCR.

A 0.8% agarose gel was prepared by melting the agarose in 1x sodium boric acid buffer (SB), adding ClearSight, pouring it into a gel apparatus and adding a comb. Since this method was only applied to assess the RNA quality approximately 250ng were mixed with 2x RNA loading dye, incubated for 5 min on 65°C and loaded onto the gel. 3µl of 1kB ladder were used and the gel was

run for approximately 35 min at 80V. Afterwards the gel was imaged in a BioRad Chemidoc with ImageLab.

6.6.3 cDNA synthesis

cDNA synthesis was performed with the iScript reverse transcription kit by BioRad. 10µg of sample RNA were mixed with 4µl of the iScript reaction mix and 1µl of iScript reverse transcriptase in a total volume of 20µl. The reaction was performed in a thermal cycler. The subsequent qPCR was performed according to the tables 6.8.1 and 6.9.2.

6.7 Statistics

Statistics were performed using GraphPad Prism 9. P-values were calculated using a two-way ANOVA with a main-effects model and Tukey's HSD test. Statistical significances are indicated for each figure.

6.8 Resource Tables

6.8.1 PCR protocols and recipe

cDNA synthesis				qPCR		
Temperature	Duration	Repetition		Temperature	Duration	Repetition
25°C	5 min	1x		95°C	15 min	1x
46°C	20 min	1x		95°C	20 sec	40x
95°C	1 min	1x		60°C	1 min	40x
4°C	∞			Melting curve For all primers without FAM probes		

component	final concentration
cDNA	2µl
$MgCl_2$ (25mM)	4mM
Primer-f (10 pmol/µl)	300nM
Primer-r (10 pmol/µl)	300nM
FAM or Evagreen (10 pmol/µl)	100nM
HotfirePol (5 U/µl)	1 U/reaction
dNTP mix (2mM each)	200µM
10x Hotfire B buffer	1x
Water	Fill up to 20µl

6.8.2 Primer for RT-qPCR

Target genes	Oligonucleotides 5'-3'
Ube2d2-Forward	AGG TCC TGT TGG AGA TGA TAT GTT
Ube2d2-Reverse	TTG GGA AAT GAA TTG TCA AGA AA
Ube2d2-fam	CCA AAT GAC AGC CCC TAT CAG GGT GG
IFNb-Forward	ATG AGT GGT GGT TGC AGG C
IFNb-Reverse	TGA CCT TTC AAA TGC AGT AGA TTC A
IFNb-fam	AAG CAT CAG AGG CGG ACT CTG GGA

panIFNa-Forward	CCA CAG GAT CAC TGT GTA CCT GAG A
panIFNa-Reverse	CTG ATC ACC TCC CAG GCA CAG
panIFNa-fam	AG[+A]A[+G]AA[+A][+C][+A]C[+A]G[+C]C

6.8.3 Antibodies for Flowcytometry

Surface marker	Fluorochrome	Company	Clone	µl used per sample and panel
B220	PerCP-Cy5.5	eBio	RA3-6B2	0.5 (B)
CD11b	Alexa F 488	eBio	M1/70	0.5 (D)
CD11b	Pb/eF 450	eBio	M1/70	1 (H)(M)
CD11b	PerCP-Cy5.5	eBio	M1/70	0.5 (L)
CD11b	PE-Cy7	eBio	M1/70	0.5 (B)
CD11c	AF700	eBio	N418	0.5 (D); 1 (M)
CD127	PE-610 (PE/Dazzle)	BioLegend	A7R34	1 (H)
CD135	PE	eBio	A2F10	1 (H)
CD150	FITC	eBio	mShad150	1 (H)
CD16/CD32	Fcg Blocking	eBio	93	0.5(B)(D)(L)(T); 1(E)(M)
CD16/CD32	PerCP-Cy5.5	eBio	93	1 (H)
CD19	APC/AF 647	eBio	eBio1D3	0.5 (L)
CD24	APC-eFluor780	eBio	M1/69	0.5 (T)
CD25	PerCP-Cy5.5	eBio	PC61.5	0.5 (T)
CD27	FITC	eBio	LG.7F9	0.5 (L)
CD317 (BST2)	PE-Cy7	eBio	eBio927	0.5 (D)
CD34	eFluor 660	eBio	RAM34	1 (H)
CD3e	Pb/eF 450	eBio	eBio500A2	0.5 (D); 1 (H)
CD3e	eFluor 506	eBio	17A2	0.5 (B)
CD3e	PE-eFluor 610	eBio	145-2C11	0.5 (L)
CD3e	PE-Cy7	eBio	145-2C11	1 (M)
CD4	Super Bright 600	eBio	GK1.5	0.5 (B)(D)(T)
CD4	PE	eBio	RM4-5	0.5 (L)
CD44	PE	eBio	IM7	0.25 (E); 0.5 (T)
CD45	AF700	Biolegend	30-F11	1 (H); 0.5 (T)
CD45R(B220)	APC/AF 647	eBio	RA3-6B2	0.5 (D)
CD45R(B220)	PE-Cy7	BioLegend	RA3-6B2	1 (M)
CD48	Super Bright 600	eBio	HM48-1	1 (H)
CD69	FITC	eBio	H1.2F3	0.5 (T)
CD8a	PE	eBio	53-6.7	0.5 (D)
CD8a	APC/AF 647	eBio	53-6.7	0.5 (B)
CD8a	Pb/eF 450	eBio	53-6.7	0.5 (L)
CD8a	PE-Cy7	eBio	53-6.7	0.5 (T)
c-KIT	APC-eFluor780	eBio	2B8	1 (H)
F4/80	FITC	eBio	BM8	1 (M)
F4/80	Pb/eF 450	eBio	BM8	1 (H)
Gr1	Pb/eF 450	eBio	RB6-8C5	1 (H)
Fixable Viability Dye	eFluor 780	eBio	-	0.5 (B)(E)(L); 1 (M)
Fixable Viability Dye	eFluor 506	eBio	-	0.5 (D)(H)(T)
Ly-6C	PerCP-Cy5.5	eBio	HK1.4	0.5 (D); 1 (M)
Ly-6G	FITC	eBio	1A8-Ly6g	0.5 (B)
Ly-6G	PE-eFluor 610	eBio	1A8-Ly6g	1 (M)
MHC II	PE	eBio	M5/114.15.2	1 (M)

Surface marker	Fluorochrome	Company	Clone	µl used per sample and panel
MHC II	APC-eFluor780	eBio	M5/114.15.2	0.5 (D)
Mouse IgM	Pb/eF 450	eBio	Eb121-15F9	0.5 (B)
NK1.1	PE	eBio	PK136	0.5 (B)
NK1.1	Pb/eF 450	eBio	PK136	0.5 (D)
NK1.1	PE-Cy7	eBio	PK136	0.5 (L); 1 (M)
Sca-1	PE-Cy7	eBio	D7	1 (H)
TCRb	Pb/eF 450	eBio	H57-597	0.5 (T)
Ter119	Pb/eF 450	eBio	TER-119	0.5 (D); 1 (E)(H)
Ter119	APC-Cy7	Biolegend	TER-119	0.5 (B)
Ter-119	PE-Cy7	eBio	Ter-119	1 (M)

***Table 1**: (B) = staining panel for blood cells; (D) = staining panel for dendritic cells; (E) = staining panel for erythroblasts; (H) = staining panel for hematopoietic stem and progenitor cells; (L) = staining panel for lymphoid cells; (M) = staining panel for myeloid cells; (T) = staining panel for thymocytes*

6.8.4 Antibodies for Western Blot

Antibody	Company	Identifier
Rabbit monoclonal anti-STAT1 (1:1000)	Cell Signaling	14995S
Rabbit monoclonal anti-STAT2 (1:500)	Cell Signaling	72604
Rabbit monoclonal anti-actin (1:1000)	Cell Signaling	9272S
Odyssey imaging systems Goat anti-Rabbit IRDye 800 CW (1:4000)	Licor Bioscience	926-32211

***Table 2**: All antibodies were diluted in TBST supplemented with 1% BSA and 0.001% NaN3, except the STAT2 antibody, for which 5% milk was used instead of BSA.*

6.8.5 Table of abbreviations

Abbreviation	Full Name
ANOVA	Analysis of Variance
APS	Ammonium Persulfate
BCA	Bicinchoninic acid
BFU-E	Burst-forming units erythroid
BM	Bone marrow
BSA	Bovine serum albumine
cDC	Classical dendritic cell
cDNA	Complementary DNA
CDP	Common dendritic precursor
CFU-GEMM	Colony-forming unit granulocyte-erythroid-macrophage-megakaryocyte
CFU-GM	Colony-forming unit granulocyte-monocyte
cGAS	Cyclic GMP–AMP
CLP	Common lymphoid precursor
CLR	C-type lectin-like receptors
CMP	Common myeloid precursor
dNTP	Deoxynucleotide triphosphate
DTT	Dithiothreitol
EDTA	Ethylenediaminetetraacetic acid
FACS	Fluorescence activated cell sorting
FAM	Fluorescein amidites
FBS	Fetal Bovine Serum
FELASA	Federation of European Laboratory Animal Science Associations
GAS	Gamma IFN-activated sites
GMP	Granulocyte-macrophage progenitors
HSC	Hematopoietic stem cell
HSD	Honestly significant difference
HSPC	Hematopietic stem and progenitor cells
IFNAR	IFN$\alpha\beta$-receptor
IFNGR	IFNγ-receptor
IFN-I	Type I interferon
IL-6	Interleukin 6
IRF	Interferon regulatory factor
ISG	Interferon stimulated genes
ISGF3	Interferon Stimulated Gene Factor 3
ISRE	IFN-stimulated response elements
IT-HSC	Intermediate-Term hematopoietic stem cell
Jak	Janus kinase
LMPP	lymphoid-myeloid primed progenitors
LSK	Lineage$^-$Sca-1$^+$c-KIT$^+$
LT-HSC	Long-Term hematopoietic stem cell
MEP	Megakaryocyte-erythroid progenitors
MkP	Megakaryocyte progenitors
MPP	Multipotent progenitors
NK cell	Natural killer cell
NLR	NOD-like receptor
NOD	Nucleotide-binding and oligomerization domain
PAGE	Polyacrylamide gel electrophoresis
PBS	Phosphate Buffered Saline

Abbreviation	Full Name
pDC	Plasmacytoid dendritic cell
PE	Phycoerythrin
PMSF	Phenylmethanesulfonylfluoride
RBC	Red blood cell
RIG-I	Retinoic acid-inducible gene I
RLR	RIG-I-like receptor
ROI	Region of interest
rpm	Rotations per minute
RPMI	Roswell Park Memorial Institute Medium
RT	Room Temperature
RT-qPCR	Reverse transcription quantitative Polymerase Chain Reaction
SB	Sodium boric acid buffer
SDS	Sodium dodecyl sulfate
SPF	Specific-pathogen-free
ST-HSC	Short-Term hematopoietic stem cell
STAT	Signal Transducer and Activator of Transcription
STING	Stimulator of interferon genes
TBST	Tris-buffered saline with Tween
TEMED	Tetramethyl ethylenediamine
TLR	Toll-like receptor
Tyk	Tyrosine kinase
WT	Wild Type

6.8.6 Table of buffers

Buffer	Contents
Flowcytometry	
Digestion Mix	RPMI + 2 % FBS, 1 mg/ml Collagenase D, 0.2 mg/ml DNase I
FACS Buffer	PBS + 1% FBS, 2.5mM EDTA, 0.02% NaN_3
Western Blot	
10x SDS-Running Buffer	144g glycin, 30g Tris base in 1l H_2O
1x SDS-Running Buffer	10x stock + 10ml SDS in 1l H_2O
SDS-PAGE Stacking Gel 5%	0.85ml acrylamide, 2.8ml H_2O, 1.25ml stacking gel buffer, 50µl 10% SDS, 50µl 10% APS, 5µl TEMED
SDS-PAGE Separating Gel 8%	2.7ml acrylamide, 4.6ml H2O, 2.5ml separating gel buffer, 100µl 10% SDS, 100µl 10% APS, 10µl TEMED
Transfer Buffer	25 mM Tris/HCl, 150 mM Glycine, 20% Methanol
Stacking gel buffer	1.5M Tris/HCl pH 8.8
Separating gel buffer	0.5M Tris/HCl pH 6.8
2x Schindler Buffer base	0.5% IGEPAL CA-630, 0.5M Tris HCl pH 8, 10% glycerol, 0.1mM EDTA pH 8, sterile filtered
1x Schindler Buffer	1x Schindler Buffer base; 0.15 M NaCl, 2mM DTT, 0.2mM Na-vanadate, 25mM NaF, 1mM PMSF, 10µg/ml Leupeptin, 0.01µg/ml Aprotinin, 1 µg/ml Pepstatin
Blocking solution	5 % milk in TBST
2x Lämmli Buffer	120mM Tris HCl pH 6.8, 4% SDS, 25% glycerin, 0.02% bromophenol blue, 20% DTT, in H_2O
10x TBS(T)	100mM Tris/HCl, 750mM NaCl, 10mM EDTA pH 8
1x TBST	10x stock, 0.1% Tween

RNA quality control	
20x SB Buffer	8g NaOH, 45g boric acid in 1l H_2O
2x RNA Loading Dye	9.5ml formamide, 50µl blue solution, 100µl 0.5M EDTA pH 8, 25µl 10% SDS in 10ml H_2O
Blue solution	0.25g bromophenol blue, 0.25g xylene cyanol in 5ml H_2O

6.8.7 Table of reagents

Reagent	Manufacturer
10X Reaction Buffer B	Solis BioDyne
Bis/-Acrylamid 37.5:1	BIO-RAD
ClearSight	Bioatlas
dNTP Mix, 10mM	Thermo Fisher
Dulbecco's Phosphate Buffered Saline (PBS)	Sigma-Aldrich
EvaGreen Dye	Biotium
Fetal bovine serum (FBS) (heat-inactivated)	Gibco
Fixation buffer	BioLegend
HOT FIREPol DNA Polymerase	Solis BioDyne
IFN-α Mouse ProcartaPlex™ Simplex Kit	Thermo Fisher
IFN-β Mouse ProcartaPlex™ Simplex Kit	Thermo Fisher
iScript cDNA Synthesis Kit	Biorad
$MgCl_2$ 25 mM	Solis BioDyne
PageRuler™ Prestained Protein Ladder	Thermo Scientific™
Pierce BCA Protein assay kit	Thermo Fisher
Ponceau S solution	Sigma-Aldrich
Procartaplex Cell Lysis Buffer (With one Roche cOmplete protease inhibitor mini tablet per 10ml and 1mM PMSF)	Invitrogen
Red Blood Cell Lysis Buffer	Sigma-Aldrich
RNA Later	Invitrogen
RPMI-1640 Medium	Sigma-Aldrich
TRIzol ™	Invitrogen™
Trypan Blue solution	Sigma-Aldrich

6.8.8 Equipment and software table

Equipment or Software	Manufacturer and model
1600 MiniG®	SPEX®sampleprep
BioRad Cell counter	TC20 Automated Cell Counter
BioRad Chemidoc	BIO-RAD Universal hood II +ImageLab software
BioRender	BioRender
Centrifuge	Rotina 420R Rotor 4784 Hettich Zentrifugen
Centrifuge	Centrifuge 5415R eppendorf
CytExpert	Beckman Coulter Life Sciences
CytoFLEX (S)	Beckman Coulter
Heat Block	Eppendorf Thermomixer 5436
Image J	National Institutes of Health
Incubator	Forma Scientific Water Jacketed Incubator 3250
Lamina	BSC-G Lab Xperts Laboratory solutions Austria
Luminex	Bio-Rad
NanoDrop 2000 Spectrophotometer	Thermo Fisher Scientific
Odyssey Imager	LI-COR Biosciences
Odyssey® Application Software	LI-COR Biosciences
PCR Machine	SimpliAmp Thermal Cycler applied biosystems
Plate Reader	Epoch BioTek
Plate Reader software	Gen5 1.11 BioTek
Power supply Gel	Power Pac 300 BIO-RAD
Power supply Transfer	Model 1000/500 Power Supply BIO-RAD
Prism 9.4.1	GraphPad Software
RT-qPCR Machine	CFX96 RealTime System C1000 Touch BIO-RAD Thermal Cycler
Semidry transfer cell	TRANS-BLOT® SD SEMI-DRY TRANSFER CELL BIO-RAD
Sonicator bath	Bandelin SONOREX RK103H
VetABC	Scil VetABC Animal Blood counter
Vortex	MS1 Minishaker IKA®

6.9 Gating strategies for Flowcytometry

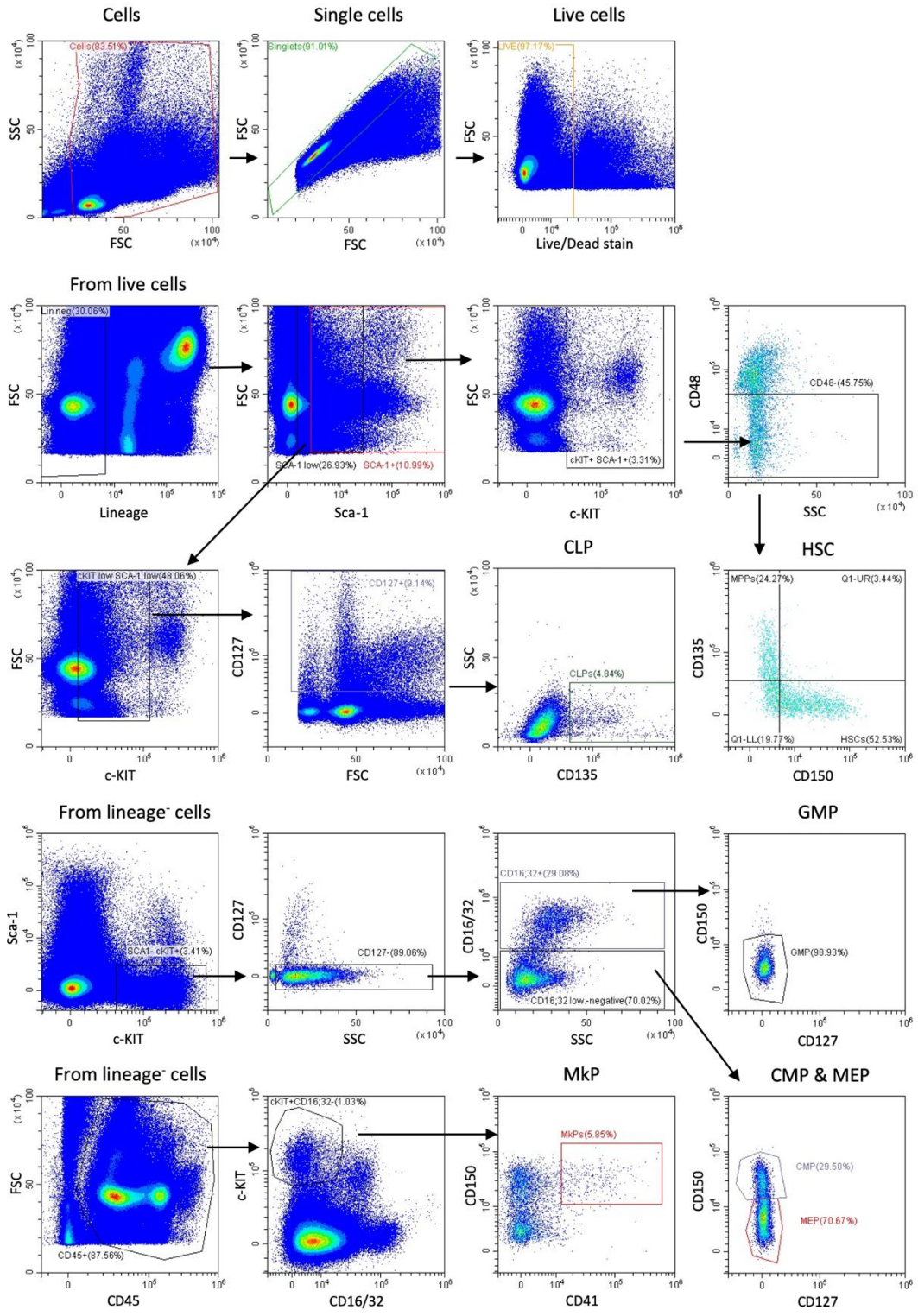

Figure 5: ***Gating strategy for hematopoietic stem and progenitor cells.*** *The first three plots represent the general gating strategy for live cells. Final populations are always labelled above the plots; arrows lead from the parent population to the subsequent plots; CLP – common lymphoid progenitors; HSC – hematopoietic stem cells; GMP – granulocyte-macrophage progenitor; MkP – megakaryocyte progenitor; CMP – common myeloid progenitor; MEP – megakaryocyte-erythroid progenitor*

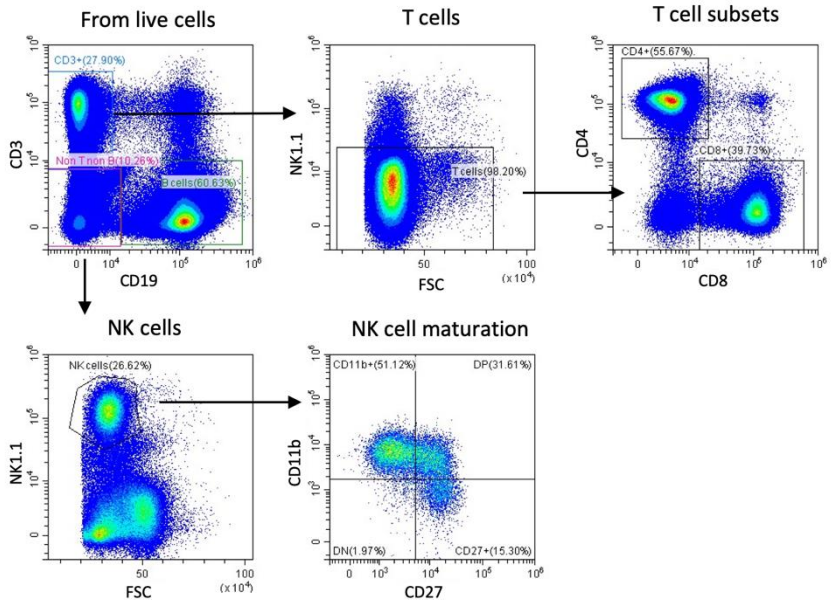

Figure 6: ***Gating strategy for lymphoid cells.*** *Gating of live cells is depicted in Figure 5; NK cells – natural killer cells*

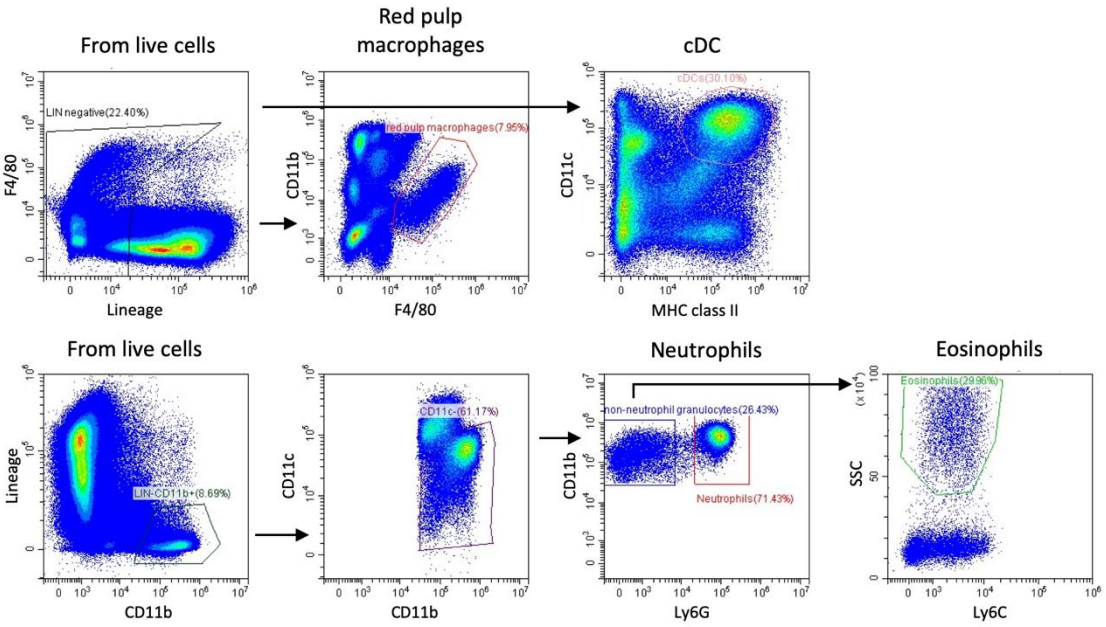

Figure 7: ***Gating strategy for myeloid cells.*** *Gating of live cells is depicted in Figure 5; cDC –classical dendritic cells*

7 Results

7.1 Mice deficient in IFNα display reduced spleen weight and splenocyte numbers

Mice lacking IFNAR1 or IFNβ are known to be fertile and produce normal sized litters. No apparent phenotypic alterations have been described and additionally, body and organ weight were reported to be comparable to WT controls (Müller et al. 1994; Hwang et al. 1995; Deonarain et al. 2003; Erlandsson et al. 1998)

During breeding and keeping in a specific-pathogen-free (SPF)-animal facility, *Ifnα*$^{-/-}$, *Ifnβ*$^{-/-}$ and IFN-I$^{-/-}$ mice showed no alterations in reproduction when compared to IFN-I$^{fl/fl}$ mice (= WT control). Furthermore, the general health checks over the course of one year, did not show any physical abnormalities: general appearance, posture, gait, and activity patterns were comparable between the four mouse lines and body weights of females and males were within the normal weight curves described for C57BL/6J mice (www.jax.org). However, of mice used in this project, 8-12-week-old *Ifnα*$^{-/-}$ mice displayed slightly reduced body weight compared to the other mutants and control mice of the same age (data not shown). Furthermore, IFN-I$^{-/-}$ and *Ifnα*$^{-/-}$ mice showed a decreased ratio of spleen weight/body weight (Figure 8A) and splenocyte numbers (Figure 8B) compared to *Ifnβ*$^{-/-}$ and IFN-I$^{fl/fl}$ mice, which were comparable to C57BL/6 mice (data not shown). Together these findings demonstrate that in contrast to IFNβ, IFNα seems to be essential for normal spleen weight and size (as observed during dissection) and splenocyte numbers.

Due to the lower number of animals used for analysis of bone marrow (BM) cell numbers, the minimal reduction seen in *Ifnα*$^{-/-}$ mice (Figure 8C) must be further evaluated to draw reliable conclusions.

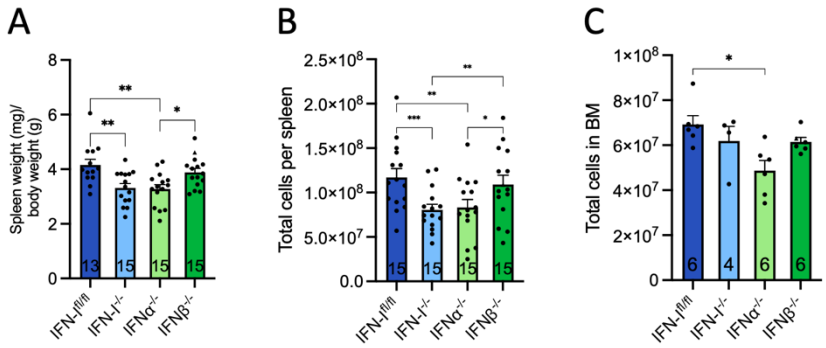

*Figure 8: **Loss of IFNα results in reduction in spleen weight and splenocyte numbers**. **A)** Spleen weight (mg) to body weight (g) ratio of 8-12-week-old IFN-I mutant and control mice **B)** Total cells per spleen and **C)** total cells in BM as determined by BioRad Cell Counter; **(A-C)** n=4-15; N=2-5; mean ± SEM are given; *p ≤ 0.05, **p ≤ 0.01, ***p ≤ 0.001; ▲=male, ●=female; n=biological replicates; N=experimental repetitions*

7.2 Lack of IFN-I results in elevated numbers of erythroid and myeloid progenitor cells

To elucidate the role of IFNα and IFNβ on hematopoiesis under steady state conditions, we initially characterized hematopoietic stem cells (HSC) isolated from the BM of *Ifnα*$^{-/-}$, *Ifnβ*$^{-/-}$, IFN-I$^{-/-}$ and their control mice by Flowcytometry. The gating strategies for HSC, progenitors and mature immune cells are depicted in Figure 5-7 (p. 30-31). Populations of hematopoietic cells are always defined as percentages out of live cells unless indicated otherwise.

In all analyzed IFN-I mutants, levels of HSCs and the size of the LSK compartment were similar to IFN-I$^{fl/fl}$ mice (Figure 9A and data not shown). However, lack of IFNα, IFNβ or both results in elevated levels of progenitors of the myeloid and erythroid lineage (Figure 9B-D) with the most pronounced increase seen in granulocyte-macrophage progenitors (GMP) (Figure 9C). Although megakaryocyte-erythroid progenitor (MEP) levels are raised in the IFN-I mutants (Figure 9D), erythroblast numbers and maturation did not differ significantly (data not shown). Furthermore, preliminary results (one experiment, three mice per genotype) show an increase in megakaryocyte progenitors (MkP) in *Ifnα*$^{-/-}$ and IFN-I$^{-/-}$ mice (data not shown).

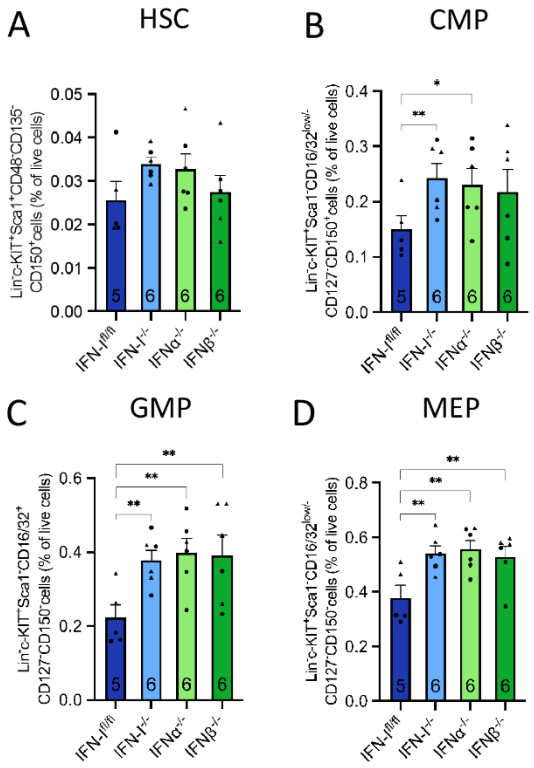

Figure 9: ***Flowcytometric analysis did not reveal noteworthy differences in HSC levels, but in progenitor cell populations. A)*** *HSC – hematopoietic stem cell;* ***B)*** *CMP – common myeloid progenitor;* ***C)*** *GMP – granulocyte-macrophage progenitor;* ***D)*** *MEP – megakaryocyte-erythroid progenitor;* ***(A-D)*** *BM cells were isolated from femur and tibia; n=5-6, N=2, mean percentages ± SEM are given; Statistical analysis was performed using a two-way ANOVA with main-effects model and Tukey's HSD test; *p ≤ 0.05, **p ≤ 0.01; ▲=male, ●=female; n=biological replicates; N=experimental repetitions*

7.3 Elevated levels of erythroid and myeloid progenitors result in unaltered mature immune cell populations

Although myeloid progenitor cells in the BM were significantly increased in *Ifnα*$^{-/-}$, *Ifnβ*$^{-/-}$ and IFN-I$^{-/-}$ mice compared to IFN-I$^{fl/fl}$ mice (Figure 9B-D), the mature populations in the blood and spleen were similar between IFN-I mutants and control mice (Figure 10A-D). Yet, there is a possible trend towards a reduction in circulating neutrophils in *Ifnα*$^{-/-}$ and *Ifnβ*$^{-/-}$ mice and an increase in splenic neutrophils in *Ifnβ*$^{-/-}$ mice (Figure 10A + C). Neutrophil numbers in the BM were similar between all genotypes and eosinophil levels in spleen and BM did not differ (data not shown).

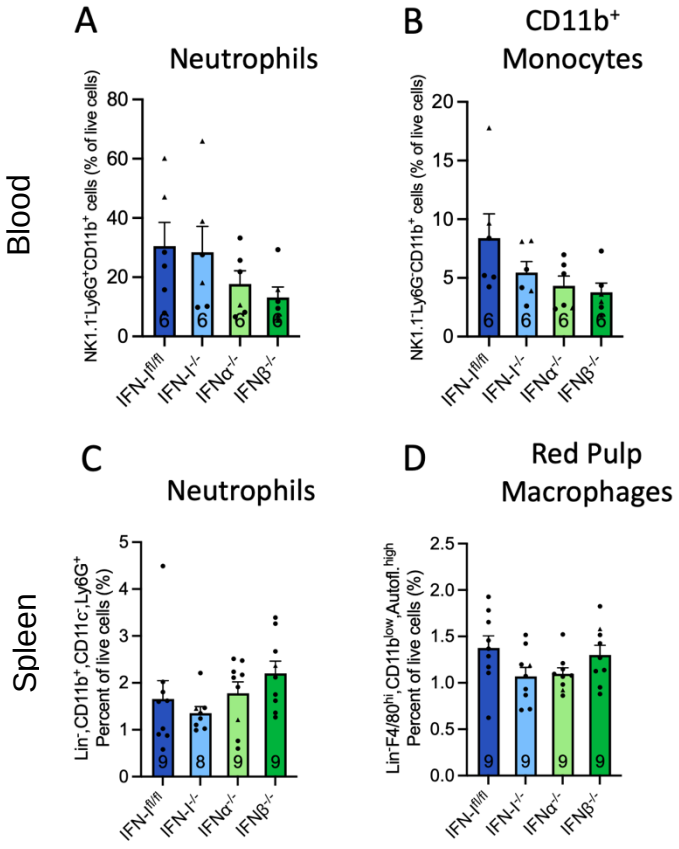

Figure 10: ***Abundance of mature myeloid lineage cells is largely unaffected by the absence of tonic IFN-I signaling. A)*** *neutrophils and* ***B)*** *CD11b⁺ monocytes in the blood;* ***C)*** *neutrophils and* ***D)*** *Red pulp macrophages in the spleen;* ***(A-D)*** *n=6-9; N=2-3; mean percentages ± SEM are given; Statistical analysis was performed using a two-way ANOVA with main-effects model and Tukey's HSD test; ▲=male, ●=female; n=biological replicates; N=experimental repetitions*

7.4 Reduction of lymphoid progenitor cells in IFN-I mutant mice has a low impact on mature T cells, B cells and DCs

In contrast to the increase in myeloid lineage progenitors seen in IFN-I mutants (Figure 9B-D), there is a significant reduction in CLPs in all IFN-I mutants (Figure 11A). This decrease is most pronounced in mice lacking both IFNα and IFNβ. To further investigate which lymphoid sub-lineages are affected from IFN-I deficiency, we analyzed T cell development in the thymus and mature populations of the lymphoid lineage in spleen, blood, and BM.

Although we did not see any differences in thymic T cell development (data not shown), total T cell numbers in the spleen of IFN-I$^{-/-}$ mice were slightly elevated compared to *Ifnα*$^{-/-}$ mice (Figure 11D). This increase is mainly attributable to the CD4^{+} subset (Figure 11E), which was increased in IFN-I$^{-/-}$ mice compared to all other mutants and control mice. The splenic CD8^{+} T cell population in contrast remained unaffected by deficiency in IFN-I (Figure 11F). In accordance with earlier work (Müller et al. 1994; Deonarain et al. 2003), the abundance of T cells and their subpopulations in the blood and BM did not differ between genotypes (data not shown).

We detected slightly elevated levels of total splenic B cells in *Ifnα*$^{-/-}$ mice (Figure 11B), however minimally lower numbers of B cells in the BM of IFN-I$^{-/-}$ mice (data not shown). Total B cell levels in the blood as well as their IgM^{+} subset, did not differ between genotypes (data not shown).

Levels of cDCs and their subsets of CD8a^{+} cDC1 and cDC2, as well as pDCs were similar between the genotypes (Figure 11C and data not shown).

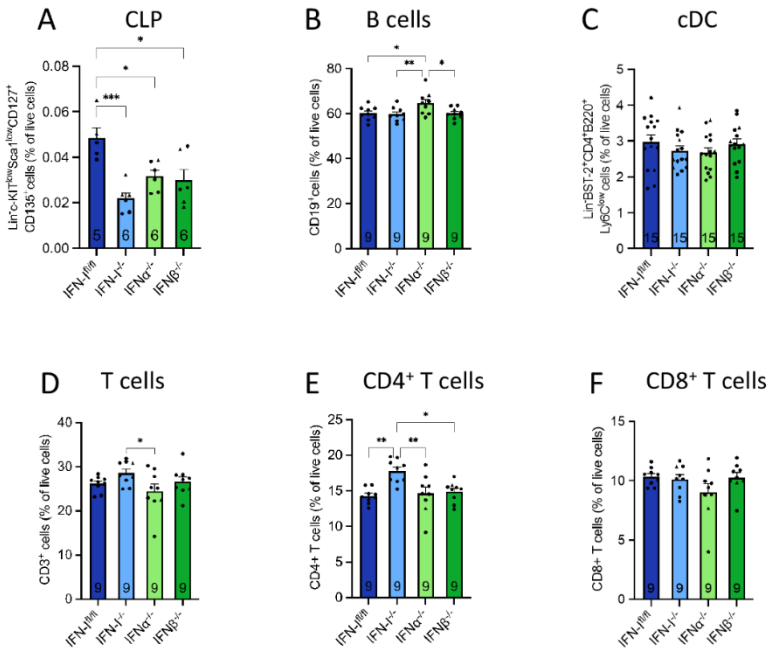

Figure 11: ***IFN-I deficiency causes strong reduction in CLPs, but exerts only minor effects on T cells, B cells and cDCs. A)*** *Common lymphoid progenitors in the BM;* ***(B-F)*** *Populations of lymphoid cells in the spleen, n=6-15, N=2-5, cDC= classical dendritic cells, CLP= common lymphoid progenitor; mean percentages ± SEM are given; Statistical analysis was performed using a two-way ANOVA with main-effects model and Tukey's HSD test; *p ≤ 0.05, **p ≤ 0.01; ***p ≤ 0.001; ▲=male, ●=female; n=biological replicates; N=experimental repetitions*

7.5 IFN-I deficiency leads to decreased NK cell numbers and impaired NK cell maturation in the spleen

In contrast to results from other lymphoid sub-lineages originating in CLPs (Figure 9B) shown above, which display only small alterations, numbers of splenic NK cells in IFN-I-mutant mice are significantly reduced (Figure 12A). The similar decrease in all IFN-I mutants suggests, that the presence of all IFN-I is required to maintain WT-levels of splenic NK cells.

Murine NK cell maturation is characterized by differential expression of the maturation markers CD11b and CD27 and divides the population into four stages: progenitors ($CD27^-CD11b^-$), immature ($CD27^+CD11b^-$), M1 mature ($CD27^+CD11b^+$) and M2 mature ($CD27^-CD11b^+$) NK cells (Chiossone et al. 2009).

Our analysis showed that IFN-Is influence NK cell maturation in spleen and BM at different stages to varying degrees. The most significant difference occurred in the M2 mature NK cells, which were reduced in IFN-$I^{-/-}$ and *Ifn*$\alpha^{-/-}$ mice (Figure 12B+D). As *Ifn*$\beta^{-/-}$ M2 NK cell levels were comparable to control NK cell levels (Figure 12B+D), we are the first to show, that IFNα is essential for the final step of NK cell maturation.

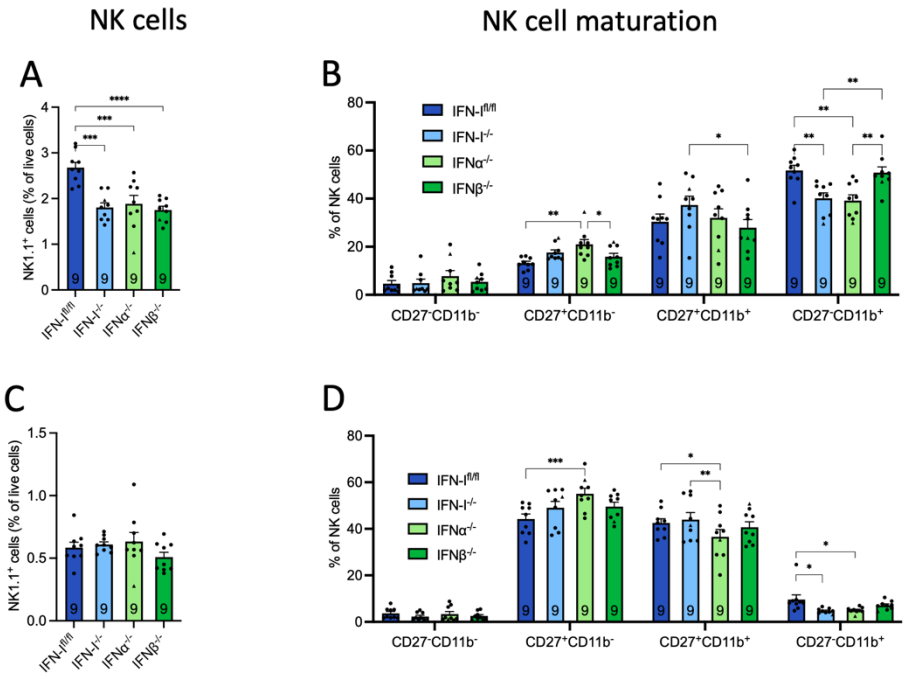

Figure 12: ***Decreased splenic NK cell numbers in IFN-I mutant mice and maturation defects in the spleen and BM upon lack of IFNα. A)*** *and* ***C)*** *NK cells in the spleen and BM defined as $CD3^-CD19^-NK1.1^+$ cells out of live cells respectively;* ***B)*** *and* ***D)*** *maturation of splenic and BM NK cells is characterized by sequential expression of the maturation markers CD27 and CD11b;* ***(A-D)*** *n=9, N=3; mean percentages ± SEM are given; Statistical analysis was performed using a two-way ANOVA with main-effects model and Tukey's HSD test; *p ≤ 0.05, **p ≤ 0.01, ***p ≤ 0.001; ****p ≤ 0.0001 ▲=male, ●=female; n=biological replicates; N=experimental repetitions*

7.6 STAT1 protein levels are affected by lack of IFNα

Tonic IFN-I is known to be essential for maintenance of appropriate levels of STAT1 and STAT2, as shown in several cell types and organs of *Ifnar1*$^{-/-}$ mice (Gough et al. 2010).

By Western Blot analysis and subsequent quantification, we could show that upon loss of IFNα, STAT1 protein levels in spleens are decreased, whereas IFNβ deficiency has no impact (Figure 13A). In the liver, STAT1 proteins were similarly lowered in the mutants compared to control mice (Figure 13B). No differences were detected in the thymus (data not shown). In spleen and liver, STAT2 protein levels are unaffected by the loss of IFN-I under homeostatic conditions (Figure 14A-B).

In addition, we could show that the ratio between STAT1α and STAT1β, as determined by quantification via ImageJ, was not altered in any of the organs (data not shown).

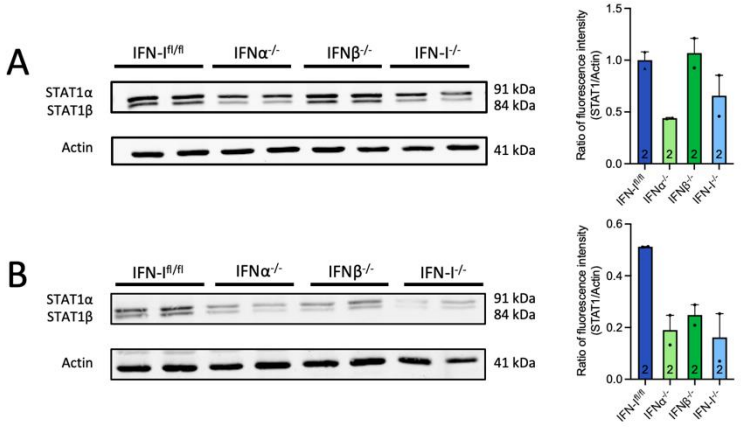

Figure 13: ***STAT1 protein levels are reduced in organs of IFN-I mutant mice****. 8µg of organ lysate were loaded onto an 8% polyacrylamide gel; STAT1 levels were determined in* ***A)*** *spleen and* ***B)*** *liver; mean percentages ± SEM are given; quantifications were performed with ImageJ software; 1 representative out of 3 experiments is shown; ▲=male, ●=female*

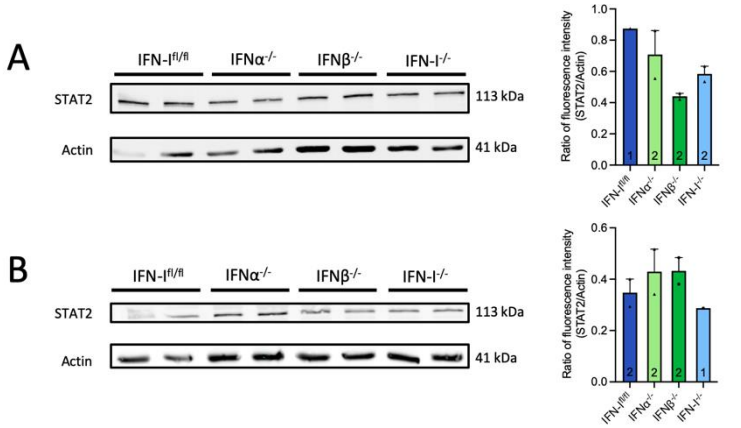

Figure 14: ***STAT2 protein levels remain largely unaffected by IFN-I deficiency.*** *8µg of organ lysate were loaded onto an 8% polyacrylamide gel; STAT2 levels were determined in* ***A)*** *spleen and* ***B)*** *liver; mean percentages ± SEM are given; quantifications were performed with ImageJ software; ▲=male, ●=female*

8 Discussion

In this study we used mice deficient in IFNα, IFNβ or both IFN-I subtypes to systematically unravel their distinct effects on hematopoiesis under steady state conditions. The two main findings of this study are a IFN-I-dependent reduction in common lymphoid progenitor (CLP) numbers and a pronounced IFN-α-dependent decrease of the most mature NK cell population.

The reduction in CLPs is caused by both, IFNα and IFNβ, as IFN-I$^{-/-}$ mice were more severely affected than the respective single mutants. An impact of IFN-Is from CLPs up to the early pro-B cell transition has already been postulated based on results from *Ifnβ*$^{-/-}$ and *Ifnar1*$^{-/-}$ mice (Mizutani et al. 2012). We are the first group to analyze CLPs in detail and showed that IFN-Is affect already the earliest progenitors of the lymphoid lineage (CLPs). The main consequences of the decreased CLP levels in IFN-I mutants are alterations in NK cells, whereas other progeny of the lymphoid lineage show minor differences in their abundance.

We detected a significant and equal reduction of total splenic NK cells in all IFN-I mutant mice, suggesting a non-additive effect of IFNα and IFNβ in upholding WT levels of NK cells in the spleen. In literature inconsistent effects of tonic IFN-I signaling on splenic NK cell abundance were described. In two studies *Ifnar1*-deficient mice displayed decreased NK cell levels (Swann et al. 2007; Mizutani et al. 2012), whereas in others splenic NK cell numbers were similar to WT levels (Guan et al. 2014; Meissl et al. 2020).

Previous studies report impaired NK cell maturation in *Ifnar1*$^{-/-}$ mice (Mizutani et al. 2012; Guan et al. 2014; Meissl et al. 2020). We are the first group to show that the reduction in the most mature (M2) NK cell population is caused mainly by lack of IFNα. While M2 NK cells of *Ifnβ*$^{-/-}$ mice were similar to WT, *Ifnα*$^{-/-}$ and IFN-I$^{-/-}$ M2 NK cells were reduced equally, leading us to the conclusion that IFNα is the main subtype in maintaining mature NK cell levels. We found a trend to an increase in the M1 stage of splenic NK cells in IFN-I$^{-/-}$ mice, as previously described in *Ifnar1*$^{-/-}$ mice (Guan et al. 2014; Meissl et al. 2020). Additionally, we discovered an increase in immature NK cells of *Ifnα*$^{-/-}$ mice, but no differences in NK cell numbers of the progenitor stage upon loss of in IFNα, IFNβ or both. In literature only isolated reports of alterations in immature and progenitor stages are available and could not be supported any further (Mizutani et al. 2012; Guan et al. 2014).

It has been shown that *Ifnar1*-deficient mice display reduced expression of STAT1 mRNA in the spleen (Gough et al. 2010). We can now confirm these results, by showing decreased splenic STAT1 levels in IFN-I mutants. This reduction was especially pronounced in mutants lacking IFNα. Furthermore, it is known that the absence of STAT1 diminishes NK cells even more and impairs their maturation (Meissl et al. 2020), leading us to propose that the alterations in NK cell numbers and in

their maturation arise from STAT1 dysregulation and consequently resemble an attenuated STAT1-deficiency.

We showed that HSC levels did not differ significantly from WT levels upon loss of IFNα, IFNβ or both. Most recent data show similar results in *Ifnar1*$^{-/-}$ mice (Li et al. 2023), whereas a slight reduction in HSCs was reported previously (Essers et al. 2009; Gui et al. 2017). Together with c-KIT and a lineage-exclusion channel, the commonly used surface marker stem cell antigen 1 (Sca-1) is used to characterize hematopoietic stem and progenitor cells (Mayle et al. 2013). It was discovered that Sca-1 is an IFN-I regulated gene (Essers et al. 2009), which was recently confirmed by analyzing CITE-Seq data from *Ifnar1*$^{-/-}$ mice (Li et al. 2023). They showed that HSC and progenitor populations differ when characterized by a few commonly used surface markers but are similar when identified via their transcriptome. Consequently, Sca-1 should not be used as a marker for HSCs anymore (Li et al. 2023).

Our remaining findings on progenitor and mature cells of the myeloid lineage are difficult to compare to the initial characterizations of *Ifnar1*$^{-/-}$ and *Ifnβ*$^{-/-}$ mice due to methodological advances within the last decades. We found common myeloid progenitors (CMPs), granulocyte-macrophage progenitors (GMPs) and megakaryocyte-erythroid progenitors (MEPs) to be increased in adult IFN-I mutant mice. Recent flowcytometric data from *Ifnar1*$^{-/-}$ mice also show an increase in GMPs and megakaryocyte progenitors (MkPs) in neonates, but these populations were described to return to WT levels within the first two weeks of life (Li et al. 2023).

Despite discovering increased myeloid progenitors in the IFN-I mutants, we found mature eosinophil, neutrophil and splenic macrophage populations to be similar to WT. Previously, macrophages and neutrophils were described to be increased in *Ifnar1*$^{-/-}$ mice (Hwang et al. 1995), whereas they were reduced in *Ifnβ*$^{-/-}$ mice (Deonarain et al. 2003). However, these results are not comparable to current data sets, as they used markers, which are no longer considered to be suitable for the identification of these populations. To identify macrophages, Mac-1 (CD11b/CD18) was used, but is now known to be expressed on macrophages, monocytes, myeloid DCs, neutrophils, granulocytes, certain B cell subsets, activated T cells and possibly also on NK cells (Erdei et al. 2019). Therefore, we identified splenic macrophages via the expression of the currently accepted surface markers F4/80, CD11b and their auto-fluorescent nature. Previously, the Gr-1 antibody/epitope was considered sufficient to identify neutrophils, however later it was discovered to stain two distinct members of the Ly6 family, namely Ly6C and Ly6G. While Ly6G is expressed highly on mature neutrophils and to a lesser degree on eosinophils and myeloid derived suppressor cells, Ly6C is more widely expressed and can be found on neutrophils, monocytes, NK cells, T cells and DCs (Lee et al.

2013). Consequently, we used CD11b, Ly6G and a lineage exclusion channel to characterize neutrophils.

In conclusion, the previous and current research on IFN-I signaling has shown that regardless of their crucial role in infections and inflammation, tonic IFN-I has surprisingly little impact on hematopoiesis under steady-state conditions. However, when investigating these subtle alterations, caution is advised as at least one commonly used surface marker has been shown to be regulated or influenced by IFN-I signaling (Essers et al. 2009; Li et al. 2023). Special attention should also be paid to housing conditions and consequently to the microbiome, which can have an impact on tonic signaling and thereby be the source of discrepancies (Schaupp et al. 2020). Further research in the field of tonic signaling is therefore expected to be based more on RNA expression analyses rather than on protein surface markers (Li et al. 2023).

Future studies should include analysis of mRNA abundance of IFN-I subtypes to discover a possible interplay between them. This could include compensatory effects or further indications to distinct functions of IFNα and IFNβ. Additionally, IFNκ should be included in this analysis, as it is still present in all IFN-I mutants and could be upregulated upon lack of IFNα or IFNβ.

Finally, the functional implications of these subtle alterations during tonic signaling, described in the newly generated IFN-I mutant mice, will become apparent when studies progress to experiments on IFN-I signaling induced by various viral or bacterial infections.

9 Acknowledgements

I would like to thank Mathias and Birgit for giving me a chance to work on this wonderful project. I had a lot of fun getting to know the world of Jak/STAT research and I grew quite attached to the topic of type I interferons over the last year. Thank you for letting me be part of such an amazing and welcoming research group.

I would like to thank my supervisors Caro and Lena for all their support and feedback in writing this thesis and of course for all the techniques they taught me and the help in long hours of flowcytometry experiments. With this in mind, I would also like to thank Jelena and Theres, who helped me handle 12 mice and up to 4 organs at once.

Furthermore, I would like to thank the whole seminar room/greenhouse crew with all my heart! You helped me through all the tough spots of the previous year and shared copious amounts of chocolate with me (and every single piece was needed). Thank you for helping me discover what team spirit can look like in the world of science. All future scientist I might work with will be held to your example. I loved to share my passion for plants with some of you and to learn so much about beautifully translated proverbs from different languages.

I would also like to thank my Mum and Grandma for supporting me during this busy year. Thank you for all the on-my-way-to-work-calls and for all the hours that you spent listening to me enthusiastically reporting every new development in my experiments (whether it made sense to you or not).

Lastly, I would like to thank Flo! Without you this year would not have been possible, let alone enjoyable. Thank you for being there for me every day and for making pudding with me after long hours in the lab. I can't wait for our next journey together.

10 References

Belyavsky, Alexander, Nataliya Petinati, and Nina Drize. 2021. “Hematopoiesis during Ontogenesis, Adult Life, and Aging.” *International Journal of Molecular Sciences* 22 (17): 9231. https://doi.org/10.3390/ijms22179231.

Borden, Ernest C., Ganes C. Sen, Gilles Uze, Robert H. Silverman, Richard M. Ransohoff, Graham R. Foster, and George R. Stark. 2007. “Interferons at Age 50: Past, Current and Future Impact on Biomedicine.” *Nature Reviews Drug Discovery* 6 (12): 975–90. https://doi.org/10.1038/nrd2422.

Caveney, Nathanael A., Robert A. Saxton, Deepa Waghray, Caleb R. Glassman, Naotaka Tsutsumi, Stevan R. Hubbard, and K. Christopher Garcia. 2023. “Structural Basis of Janus Kinase Trans-Activation.” *Cell Reports* 42 (3). https://doi.org/10.1016/j.celrep.2023.112201.

Chen, James C., Mariano J. Alvarez, Flaminia Talos, Harshil Dhruv, Gabrielle E. Rieckhof, Archana Iyer, Kristin L. Diefes, et al. 2014. “Identification of Causal Genetic Drivers of Human Disease through Systems-Level Analysis of Regulatory Networks.” *Cell* 159 (2): 402–14. https://doi.org/10.1016/j.cell.2014.09.021.

Chiossone, Laura, Julie Chaix, Nicolas Fuseri, Claude Roth, Eric Vivier, and Thierry Walzer. 2009. “Maturation of Mouse NK Cells Is a 4-Stage Developmental Program.” *Blood* 113 (22): 5488–96. https://doi.org/10.1182/blood-2008-10-187179.

Crow, Yanick J., and Daniel B. Stetson. 2022. “The Type I Interferonopathies: 10 Years On.” *Nature Reviews. Immunology* 22 (8): 471–83. https://doi.org/10.1038/s41577-021-00633-9.

Decker, Thomas, Mathias Müller, and Silvia Stockinger. 2005. “The Yin and Yang of Type I Interferon Activity in Bacterial Infection.” *Nature Reviews Immunology* 5 (9): 675–87. https://doi.org/10.1038/nri1684.

Deonarain, Raj, Antonio Alcamí, Maria Alexiou, Margaret J. Dallman, Dirk R. Gewert, and Andrew C. G. Porter. 2000. “Impaired Antiviral Response and Alpha/Beta Interferon Induction in Mice Lacking Beta Interferon.” *Journal of Virology* 74 (7): 3404–9. https://doi.org/10.1128/JVI.74.7.3404-3409.2000.

Deonarain, Raj, Amit Verma, Andrew C. G. Porter, Dirk R. Gewert, Leonidas C. Platanias, and Eleanor N. Fish. 2003. “Critical Roles for IFN-β in Lymphoid Development, Myelopoiesis, and Tumor Development: Links to Tumor Necrosis Factor α.” *Proceedings of the National Academy of Sciences of the United States of America* 100 (23): 13453–58. https://doi.org/10.1073/pnas.2230460100.

Erdei, Anna, Szilvia Lukácsi, Bernadett Mácsik-Valent, Zsuzsa Nagy-Baló, István Kurucz, and Zsuzsa Bajtay. 2019. “Non-Identical Twins: Different Faces of CR3 and CR4 in Myeloid and Lymphoid Cells of Mice and Men.” *Seminars in Cell & Developmental Biology*, Axon guidance: Signaling pathways old and new across a variety of developmental contexts, 85 (January): 110–21. https://doi.org/10.1016/j.semcdb.2017.11.025.

Erlandsson, Lena, Ralf Blumenthal, Maija-Leena Eloranta, Holger Engel, Gunnar Alm, Siegfried Weiss, and Tomas Leanderson. 1998. “Interferon-β Is Required for Interferon-α Production in Mouse Fibroblasts.” *Current Biology* 8 (4): 223–26. https://doi.org/10.1016/S0960-9822(98)70086-7.

Essers, Marieke A. G., Sandra Offner, William E. Blanco-Bose, Zoe Waibler, Ulrich Kalinke, Michel A. Duchosal, and Andreas Trumpp. 2009. “IFNα Activates Dormant Haematopoietic Stem Cells in Vivo.” *Nature* 458 (7240): 904–8. https://doi.org/10.1038/nature07815.

Fenner, Jennifer E., Robyn Starr, Ann L. Cornish, Jian-Guo Zhang, Donald Metcalf, Robert D. Schreiber, Kathleen Sheehan, Douglas J. Hilton, Warren S. Alexander, and Paul J. Hertzog. 2006. “Suppressor of Cytokine Signaling 1 Regulates the Immune Response to Infection by a Unique Inhibition of Type I Interferon Activity.” *Nature Immunology* 7 (1): 33–39. https://doi.org/10.1038/ni1287.

Ferrari, Giuliana, Adrian J. Thrasher, and Alessandro Aiuti. 2021. “Gene Therapy Using Haematopoietic Stem and Progenitor Cells.” *Nature Reviews Genetics* 22 (4): 216–34. https://doi.org/10.1038/s41576-020-00298-5.

Fleetwood, Andrew J., Hang Dinh, Andrew D. Cook, Paul J Hertzog, and John A. Hamilton. 2009. “GM-CSF- and M-CSF-Dependent Macrophage Phenotypes Display Differential Dependence on Type I Interferon Signaling.” *Journal of Leukocyte Biology* 86 (2): 411–21. https://doi.org/10.1189/jlb.1108702.

Fox, Lindsey E., Marissa C. Locke, and Deborah J. Lenschow. 2020. “Context Is Key: Delineating the Unique Functions of IFNα and IFNβ in Disease.” *Frontiers in Immunology* 11. https://www.frontiersin.org/articles/10.3389/fimmu.2020.606874.

Gough, Daniel J., Nicole L. Messina, Christopher J. P. Clarke, Ricky W. Johnstone, and David E. Levy. 2012. “Constitutive Type I Interferon Modulates Homeostatic Balance through Tonic Signaling.” *Immunity* 36 (2): 166–74. https://doi.org/10.1016/j.immuni.2012.01.011.

Gough, Daniel J., Nicole L. Messina, Linda Hii, Jodee A. Gould, Kanaga Sabapathy, Ashley P. S. Robertson, Joseph A. Trapani, et al. 2010. “Functional Crosstalk between Type I and II Interferon through the Regulated Expression of STAT1.” *PLoS Biology* 8 (4): e1000361. https://doi.org/10.1371/journal.pbio.1000361.

Guan, Jean, S. M. Shahjahan Miah, Zachary S. Wilson, Timothy K. Erick, Cindy Banh, and Laurent Brossay. 2014. “Role of Type I Interferon Receptor Signaling on NK Cell Development and Functions.” *PLOS ONE* 9 (10): e111302. https://doi.org/10.1371/journal.pone.0111302.

Gui, Jun, Bin Zhao, Kaosheng Lyu, Wei Tong, and Serge Y. Fuchs. 2017. “Downregulation of the IFNAR1 Chain of Type 1 Interferon Receptor Contributes to the Maintenance of the Haematopoietic Stem Cells.” *Cancer Biology & Therapy* 18 (7): 534–43. https://doi.org/10.1080/15384047.2017.1345395.

Hardy, Matthew P., Catherine M. Owczarek, Lars S. Jermiin, Mikael Ejdebäck, and Paul J. Hertzog. 2004. “Characterization of the Type I Interferon Locus and Identification of Novel Genes.” *Genomics* 84 (2): 331–45. https://doi.org/10.1016/j.ygeno.2004.03.003.

Hwang, S Y, P J Hertzog, K A Holland, S H Sumarsono, M J Tymms, J A Hamilton, G Whitty, I Bertoncello, and I Kola. 1995. “A Null Mutation in the Gene Encoding a Type I Interferon Receptor Component Eliminates Antiproliferative and Antiviral Responses to Interferons Alpha and Beta and Alters Macrophage Responses.” *Proceedings of the National Academy of Sciences* 92 (24): 11284–88. https://doi.org/10.1073/pnas.92.24.11284.

Isaacs, A., and J. Lindenmann. 1957. “Virus Interference. I. The Interferon.” *Proceedings of the Royal Society of London. Series B, Biological Sciences* 147 (927): 258–67. https://doi.org/10.1098/rspb.1957.0048.

Kennedy, Mary K., Moira Glaccum, Sandra N. Brown, Eric A. Butz, Joanne L. Viney, Monica Embers, Naoto Matsuki, et al. 2000. “Reversible Defects in Natural Killer and Memory Cd8 T Cell Lineages in Interleukin 15–Deficient Mice.” *Journal of Experimental Medicine* 191 (5): 771–80. https://doi.org/10.1084/jem.191.5.771.

Kernbauer, Elisabeth, Verena Maier, Isabella Rauch, Mathias Müller, and Thomas Decker. 2013. “Route of Infection Determines the Impact of Type I Interferons on Innate Immunity to Listeria Monocytogenes.” *PLOS ONE* 8 (6): e65007. https://doi.org/10.1371/journal.pone.0065007.

Kotenko, Sergei V., Amariliz Rivera, Dane Parker, and Joan E. Durbin. 2019. “Type III IFNs: Beyond Antiviral Protection.” *Seminars in Immunology* 43 (June): 101303. https://doi.org/10.1016/j.smim.2019.101303.

Kovarik, Pavel, Virginia Castiglia, Masa Ivin, and Florian Ebner. 2016. “Type I Interferons in Bacterial Infections: A Balancing Act.” *Frontiers in Immunology* 7. https://www.frontiersin.org/articles/10.3389/fimmu.2016.00652.

Lee, Pui Y., Jun-Xia Wang, Emilio Parisini, Christopher C. Dascher, and Peter A. Nigrovic. 2013. “Ly6 Family Proteins in Neutrophil Biology.” *Journal of Leukocyte Biology* 94 (4): 585–94. https://doi.org/10.1189/jlb.0113014.

Li, Yanan, Wei Yang, Helen C. Wang, Riddhi M. Patel, Emily B. Casey, Elisabeth D Denby, and Jeffrey A Magee. 2023. “Basal Type I Interferon Signaling Has Only Modest Effects on Neonatal and Juvenile Hematopoiesis.” *Blood Advances*, February, bloodadvances.2022008595. https://doi.org/10.1182/bloodadvances.2022008595.

Lu, Yi-Chien, Chad Sanada, Juliana Xavier-Ferrucio, Lin Wang, Ping-Xia Zhang, H. Leighton Grimes, Meenakshi Venkatasubramanian, et al. 2018. “The Molecular Signature of Megakaryocyte-Erythroid Progenitors Reveals a Role for the Cell Cycle in Fate Specification.” *Cell Reports* 25 (8): 2083-2093.e4. https://doi.org/10.1016/j.celrep.2018.10.084.

Mattei, Fabrizio, Giovanna Schiavoni, Filippo Belardelli, and David F. Tough. 2001. “IL-15 Is Expressed by Dendritic Cells in Response to Type I IFN, Double-Stranded RNA, or Lipopolysaccharide and Promotes Dendritic Cell Activation1.” *The Journal of Immunology* 167 (3): 1179–87. https://doi.org/10.4049/jimmunol.167.3.1179.

Mayle, Allison, Min Luo, Mira Jeong, and Margaret A. Goodell. 2013. “Mouse Hematopoietic Stem Cell Identification And Analysis.” *Cytometry. Part A : The Journal of the International Society for Analytical Cytology* 83 (1): 27–37. https://doi.org/10.1002/cyto.a.22093.

Meissl, Katrin, Natalija Simonović, Lena Amenitsch, Agnieszka Witalisz-Siepracka, Klara Klein, Caroline Lassnig, Ana Puga, et al. 2020. “STAT1 Isoforms Differentially Regulate NK Cell Maturation and Anti-Tumor Activity.” *Frontiers in Immunology* 11 (September): 2189. https://doi.org/10.3389/fimmu.2020.02189.

Mizutani, Tatsuaki, Nina Neugebauer, Eva M. Putz, Nadine Moritz, Olivia Simma, Eva Zebedin-Brandl, Dagmar Gotthardt, et al. 2012. “Conditional IFNAR1 Ablation Reveals Distinct Requirements of Type I IFN Signaling for NK Cell Maturation and Tumor Surveillance.” *OncoImmunology* 1 (7): 1027–37. https://doi.org/10.4161/onci.21284.

Müller, Ulrike, Ulrich Steinhoff, Luiz F. L. Reis, Silvio Hemmi, Jovan Pavlovic, Rolf M. Zinkernagel, and Michel Aguet. 1994. “Functional Role of Type I and Type II Interferons in Antiviral Defense.” *Science* 264 (5167): 1918–21. https://doi.org/10.1126/science.8009221.

Pesch, Vincent van, and Thomas Michiels. 2003. “Characterization of Interferon-Alpha 13, a Novel Constitutive Murine Interferon-Alpha Subtype.” *The Journal of Biological Chemistry* 278 (47): 46321–28. https://doi.org/10.1074/jbc.M302554200.

Platanias, Leonidas C. 2005. “Mechanisms of Type-I- and Type-II-Interferon-Mediated Signalling.” *Nature Reviews Immunology* 5 (5): 375–86. https://doi.org/10.1038/nri1604.

Sato, Taku, Nobuyuki Onai, Hiroki Yoshihara, Fumio Arai, Toshio Suda, and Toshiaki Ohteki. 2009. “Interferon Regulatory Factor-2 Protects Quiescent Hematopoietic Stem Cells from Type I Interferon–Dependent Exhaustion.” *Nature Medicine* 15 (6): 696–700. https://doi.org/10.1038/nm.1973.

Schaupp, Laura, Sabine Muth, Leif Rogell, Michael Kofoed-Branzk, Felix Melchior, Stefan Lienenklaus, Stephanie C. Ganal-Vonarburg, et al. 2020. “Microbiota-Induced Type I Interferons Instruct a Poised Basal State of Dendritic Cells.” *Cell* 181 (5): 1080-1096.e19. https://doi.org/10.1016/j.cell.2020.04.022.

Schreiber, Gideon. 2017. “The Molecular Basis for Differential Type I Interferon Signaling.” *Journal of Biological Chemistry* 292 (18): 7285–94. https://doi.org/10.1074/jbc.R116.774562.

Shepardson, Kelly M., Kyle Larson, Laura L. Johns, Kayla Stanek, Hanbyul Cho, Julia Wellham, Haley Henderson, and Agnieszka Rynda-Apple. 2018. “IFNAR2 Is Required for Anti-Influenza Immunity and Alters Susceptibility to Post-Influenza Bacterial Superinfections.” *Frontiers in Immunology* 9. https://www.frontiersin.org/articles/10.3389/fimmu.2018.02589.

Swann, Jeremy B., Yoshihiro Hayakawa, Nadeen Zerafa, Kathleen C. F. Sheehan, Bernadette Scott, Robert D. Schreiber, Paul Hertzog, and Mark J. Smyth. 2007. “Type I IFN Contributes to NK Cell Homeostasis, Activation, and Antitumor Function1.” *The Journal of Immunology* 178 (12): 7540–49. https://doi.org/10.4049/jimmunol.178.12.7540.

Swiecki, Melissa, and Marco Colonna. 2011. “Type I Interferons: Diversity of Sources, Production Pathways and Effects on Immune Responses.” *Current Opinion in Virology*, Innate

immunity/Antivirals and resistance/Emerging viruses, 1 (6): 463–75. https://doi.org/10.1016/j.coviro.2011.10.026.

Takaoka, A., Y. Mitani, H. Suemori, M. Sato, T. Yokochi, S. Noguchi, N. Tanaka, and T. Taniguchi. 2000. "Cross Talk between Interferon-Gamma and -Alpha/Beta Signaling Components in Caveolar Membrane Domains." *Science (New York, N.Y.)* 288 (5475): 2357–60. https://doi.org/10.1126/science.288.5475.2357.

Taniguchi, Tadatsugu, and Akinori Takaoka. 2001. "A Weak Signal for Strong Responses: Interferon-Alpha/Beta Revisited." *Nature Reviews Molecular Cell Biology* 2 (5): 378–86. https://doi.org/10.1038/35073080.

Tovey, M G, M Streuli, I Gresser, J Gugenheim, B Blanchard, J Guymarho, F Vignaux, and M Gigou. 1987. "Interferon Messenger RNA Is Produced Constitutively in the Organs of Normal Individuals." *Proceedings of the National Academy of Sciences of the United States of America* 84 (14): 5038–42.

Vasconcellos, Rita, Deborah Braun, Antonio Coutinho, and Jocelyne Demengeot. 1999. "Type I IFN Sets the Stringency of B Cell Repertoire Selection in the Bone Marrow." *International Immunology* 11 (2): 279–88. https://doi.org/10.1093/intimm/11.2.279.

Yu, Le, and Pengda Liu. 2021. "Cytosolic DNA Sensing by CGAS: Regulation, Function, and Human Diseases." *Signal Transduction and Targeted Therapy* 6 (1): 1–15. https://doi.org/10.1038/s41392-021-00554-y.

Zhang, Yifan, Shuai Gao, Jun Xia, and Feng Liu. 2018. "Hematopoietic Hierarchy – An Updated Roadmap." *Trends in Cell Biology*, Special Issue: Stem Cell Biology, 28 (12): 976–86. https://doi.org/10.1016/j.tcb.2018.06.001.